Designing Dual Inhibitors of Anaplastic Lymphoma Kinase (ALK) and Bromodomain-4 (BRD4) by Tuning Kinase Selectivity

Ellen Watts,[†] David Heidenreich,[‡,§] Elizabeth Tucker,[||] Monika Raab,[⊥] Klaus Strebhardt,[⊥] Louis Chesler,[||] Stefan Knapp,[‡,§,#] Benjamin Bellenie,*,[†] and Swen Hoelder*,[†]

[†]Cancer Research UK Cancer Therapeutics Unit at The Institute of Cancer Research, London SM2 5NG, U.K.

[‡]Institute for Pharmaceutical Chemistry, Johann Wolfgang Goethe-University, Max-von-Laue-Strasse 9, D-60438 Frankfurt am Main, Germany

[§]Structural Genomics Consortium, BMLS, Goethe-University Frankfurt, 60438 Frankfurt, Germany
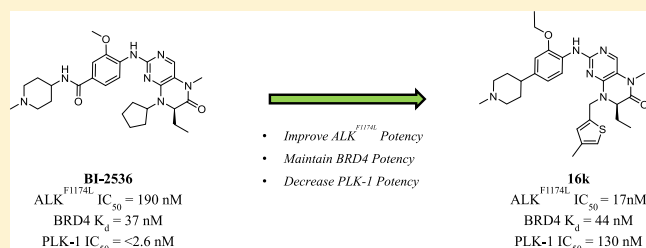
[||]Paediatric and Solid Tumour Biology and Therapeutics Group, The Institute of Cancer Research, 15 Cotswold Road, London SM2 5NG, U.K.

[⊥]Department of Gynecology and Obstetrics, Johann Wolfgang Goethe-University, Theodor-Stern Kai 7, 60590 Frankfurt am Main, Germany

[#]German Cancer Network (DKTK), Site Frankfurt/Mainz, D-60438 Frankfurt am Main, Germany

S Supporting Information

ABSTRACT: Concomitant inhibition of anaplastic lymphoma kinase (ALK) and bromodomain-4 (BRD4) is a potential therapeutic strategy for targeting two key oncogenic drivers that co-segregate in a significant fraction of high-risk neuroblastoma patients, mutation of ALK and amplification of *MYCN*. Starting from known dual polo-like kinase (PLK)-1−BRD4 inhibitor BI-2536, we employed structure-based design to redesign this series toward compounds with a dual ALK−BRD4 profile. These efforts led to compound (*R*)-2-((2-ethoxy-4-(1-methylpiperidin-4-yl)phenyl)amino)-7-ethyl-5-methyl-8-((4-methylthiophen-2-yl)methyl)-7,8-dihydropteridin-6(5*H*)-one (**16k**) demonstrating improved ALK activity and significantly reduced PLK-1 activity, while maintaining BRD4 activity and overall kinome selectivity. We demonstrate the compounds' on-target engagement with ALK and BRD4 in cells as well as favorable broad kinase and bromodomain selectivity.

BI-2536
ALK^{F1174L} IC$_{50}$ = 190 nM
BRD4 K$_d$ = 37 nM
PLK-1 IC$_{50}$ = <2.6 nM

- *Improve ALK^{F1174L} Potency*
- *Maintain BRD4 Potency*
- *Decrease PLK-1 Potency*

16k
ALK^{F1174L} IC$_{50}$ = 17nM
BRD4 K$_d$ = 44 nM
PLK-1 IC$_{50}$ = 130 nM

INTRODUCTION

Neuroblastoma is a pediatric cancer of neural crest origin and is the most common extracranial solid tumor in childhood.[1] In high-risk patients, mutations within the kinase domain of the anaplastic lymphoma kinase (ALK), such as ALK^{F1174L}, co-segregate with amplification of the *MYCN* gene. Since the ALK mutation increases transcription and expression of MYCN, both oncogenic gene changes cooperate to upregulate this well-established driver of neuroblastoma proliferation, resulting in poor prognosis and clinical outcome.[2]

Several selective inhibitors of the ALK kinase have been disclosed and entered clinical trials for different indications. However, crizotinib is clinically ineffective in neuroblastoma and many second-generation ALK inhibitors are predicted to be ineffective for neuroblastoma patients harboring the F1174L mutation due to insufficient inhibition of the mutant kinase.[3] Recently, the third-generation ALK inhibitor lorlatinib was shown to potently inhibit ALK^{F1174L} and has now entered phase I clinical trials in relapsed or refractory neuroblastoma patients.[4]

Inhibition of bromodomain-4 (BRD4) has recently emerged as an essential transcriptional co-regulator of MYCN, and inhibition of the bromodomain has been shown to be an effective therapeutic approach to target dysregulated *MYCN* in neuroblastoma.[5−7] Several compounds have progressed to clinical trials for adult malignancies but have yet to reach pediatric trials.[8,9]

It is increasingly recognized that targeting multiple pathways that support cancer growth and survival is necessary to treat aggressive cancers, provide a more durable response, and overcome resistance.[10] Given the clinical challenge that high-risk neuroblastoma cases pose, combining ALK and BRD4 inhibition may represent an effective therapeutic approach for this high medical need. Combining both ALK and BRD4 inhibition would serve two purposes. First, it would target the two most common and co-segregating events that drive high-risk neuroblastoma and curb *MYCN* expression, potentially resulting in strong antiproliferative or proapoptopic effects. Moreover, blocking two targets at once reduces the risk of resistance to the therapy since the probability of clonal

Hinge binding region

KAc Mimetic

ALK^{F1174L} IC$_{50}$: 190 nM
ALK WT IC$_{50}$: 390 nM
BRD4(1) K$_{d}$: 37 nM
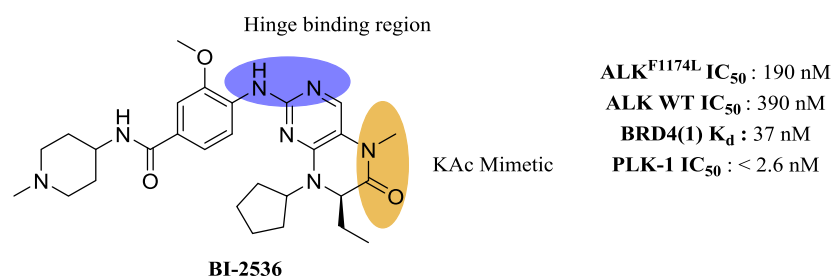**PLK-1 IC$_{50}$** : < 2.6 nM

BI-2536

Figure 1. Biochemical potencies of the dual PLK-1−BRD4 inhibitor BI-2536 and moieties of the molecule that form key interactions with BRD4 (orange) and the PLK-1 hinge region (violet).
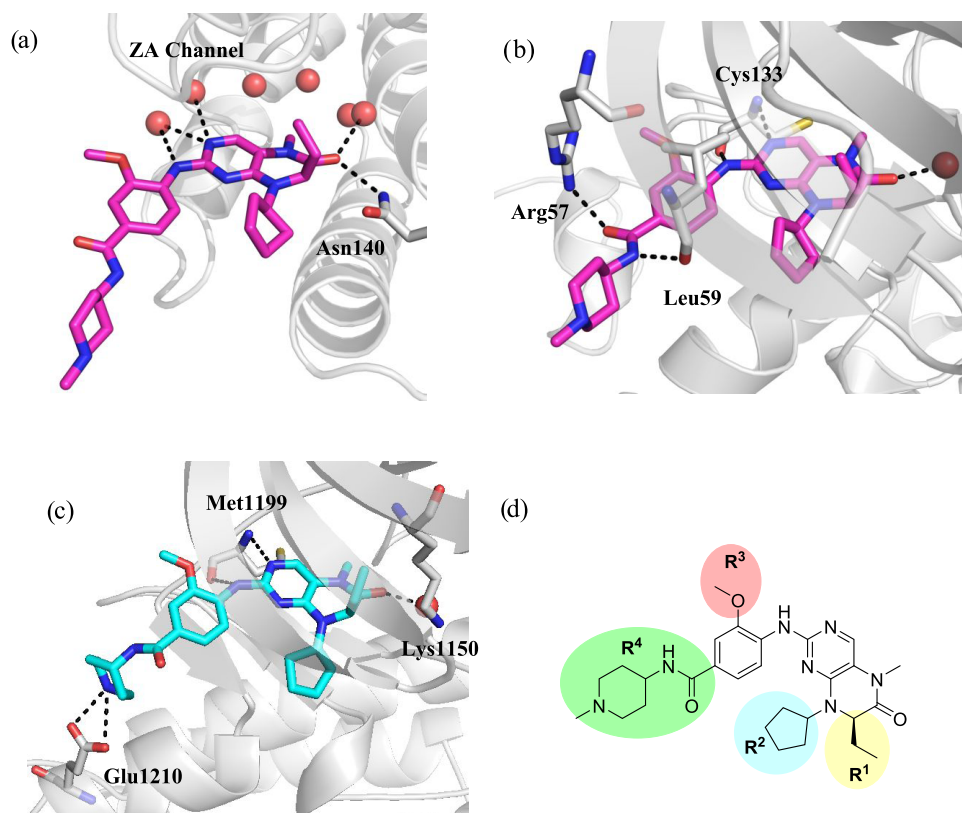

Figure 2. X-ray structures of BI-2536 in complex with (a) BRD4 (4OGI) and (b) PLK-1 (2RKU) highlighting key interactions. (c) Docking pose generated using Glide showing BI-2536 in complex with ALK (2XB7), highlighting key interactions. (d) Four chosen areas for modification on BI-2536.

adaptation to targeted therapy is lower for combination therapies.[11]

A key barrier in clinical implementation of new agents or treatment strategies in children is that combination trials of multiple drugs are challenging in pediatric patients. This is in part due to the increased chance of off-target toxicity when two agents are tested and length of trials because tolerable dose must be established for each new agent separately in very small patient populations.

An alternative approach to using two drugs in combination is to explore dual inhibitors that block both targets of a therapeutic combination, in the case of high-risk neuroblastoma, BRD4 and ALK^{F1174L}. A dual inhibitor is likely to reduce the liabilities associated with combination treatments, particularly, off-target toxicities, drug−drug interactions, and additive effects. Furthermore, combinatorial treatment in the form of a dual inhibitor reduces the length and complexity of trials as well as costs.[10,12,13]

Dual inhibitors are thus an attractive therapeutic approach, but the design and development of drugs that specifically inhibit two targets, particularly, where these are structurally distinct and not members of the same protein family, are challenging. In particular, combining two pharmacophores into a single druglike compound while also achieving selectivity and physicochemical and pharmacokinetics properties consistent with clinical development is regarded as very difficult.[10]

However, precedent for dual kinase−bromodomain inhibitors has recently emerged. Through systematic screening efforts, Ember et al. and Ciceri et al. identified a total of 24 kinase inhibitors that interact with BRD4.[14,15] Cocrystal structures of these dual inhibitors revealed insights into how the BRD4 and kinase pharmacophores can be combined into a single druglike molecule. Although these reports provide important precedence for dual kinase−bromodomain inhibition and structural insights, the combination of bromodomain and kinase inhibited by these dual inhibitors was discovered

B

Scheme 1
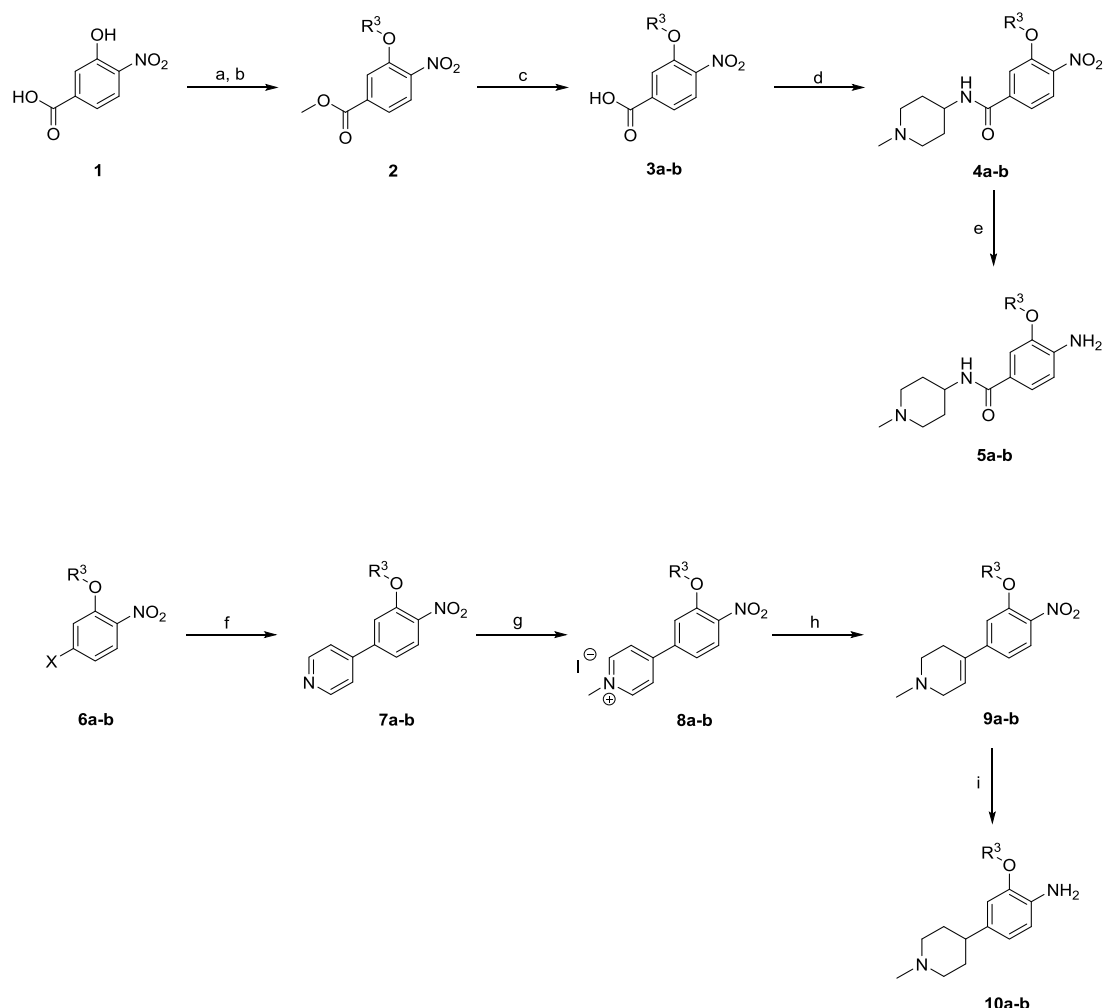
^{a}Reagents and conditions: (a) SOCl$_2$, MeOH, 70 °C, 90%; (b) 1-iodo-2-methylpropane, K$_2$CO$_3$, dimethylformamide (DMF), 50 °C, 88%; (c) LiOH, H$_2$O, room temperature (rt), 71%; (d) 4-amino-1-methylpiperidine, HBTU, Et$_3$N, DMF, rt, 77−86%; (e) SnCl$_2$·2H$_2$O, EtOAc/EtOH, 10:3, 50 °C, 53−55%; (f) 4-pyridylboronic acid, PdCl$_2$(PPh$_3$)$_2$, Na$_2$CO$_3$, dioxane/water 6:1, 110 °C, 54−65%; (g) MeI, MeCN, 50 °C, 91−99%; (h) NaBH$_4$, MeOH, rt, 56−95%; (i) H$_2$, PtO$_2$, AcOH, 50 psi, 75−85%.

serendipitously by screening selective kinase inhibitors against the bromo- and extra-terminal domain (BET) bromodomains. To date, there are a few published reports of discovery efforts that aim to combine inhibition of a particular kinase with bromodomain inhibition into a single dual inhibitor to explore a specific disease hypothesis.[16−18]

Herein, we describe our efforts to discover dual ALK−BRD4 inhibitors to target both oncogenic drivers of high-risk neuroblastoma. We chose the dual polo-like kinase (PLK)-1−BRD4 inhibitor BI-2536 as our starting point and investigated if this inhibitor series can be reoptimized to show potent inhibition of mutant (F1174L) ALK kinase, reduced PLK-1 activity while maintaining BRD4 activity, and acceptable kinome selectivity.

RESULTS AND DISCUSSION

Our goal at the start of the project was to discover starting points that showed significant activity against BRD4 and the ALK kinase. We were particularly intrigued by the dual kinase−bromodomain inhibitor BI-2536 (Figure 1). The compound was discovered and developed as a PLK-1 kinase inhibitor but was found to potently inhibit BRD4 by Knapp

and Schönbrunn's labs.[14,19,20] BI-2536 has been reported to show high specificity within the kinase family, partially due to the methoxy substituent. Some kinases are not able to accommodate this substituent due to a steric clash with a larger tyrosine or tryptophan residue in the hinge region. Among the exceptions are PLK-1 and importantly ALK due to the presence of a smaller leucine at this position.[21,22] We thus hypothesized that although BI-2536 showed excellent overall kinase selectivity it may show sufficient activity against ALK and ALK^{F1174L} to serve as a starting point. We analyzed the publicly available data, and indeed a K_d of 160 nM had been disclosed for ALK.[23] In our assays, BI-2536 showed comparable, albeit modest, activity (IC$_{50}$s of 390 and 190 nM against ALK and ALK^{F1174L}, respectively).

In addition, we confirmed inhibition of BRD4 and PLK-1. In fact, the potency of BI-2536 against PLK-1 was beyond the dynamic range of the assay (IC$_{50}$ < 2.6 nM) consistent with a published K_d of 0.19 nM.[23]

BI-2536 thus was a suitable starting point for the discovery of a dual ALK−BRD4 inhibitor, not least because it inhibited a few other kinases apart from PLK-1 and ALK.[23] We thus decided to investigate if BI-2536 can be optimized toward a

Scheme 2
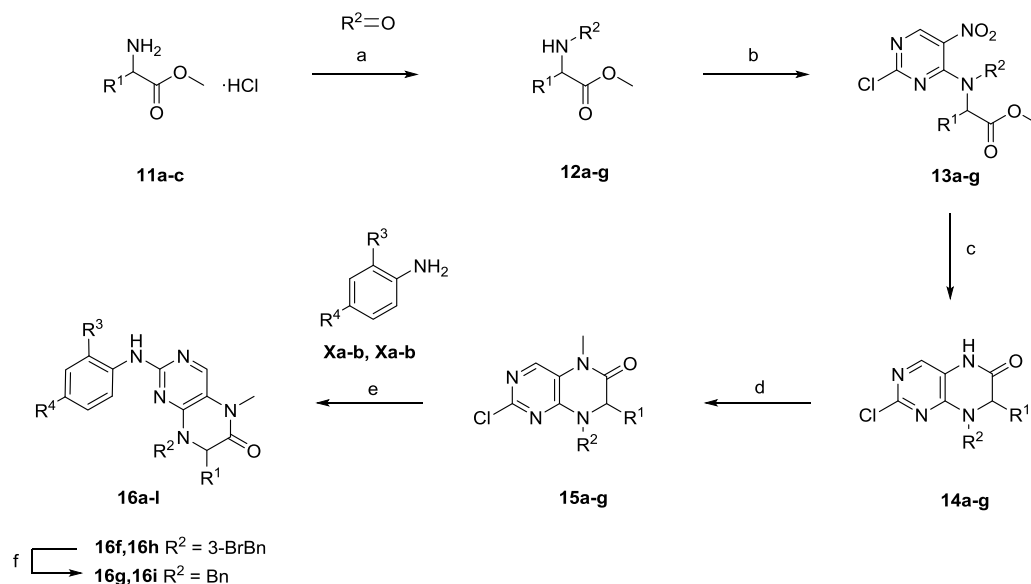
[a]Reagents and conditions: (a) NaBH(OAc)$_3$, NaOAc, 1,2-dichloroethane (DCE), rt, 16 h, 39−94%; (b) 2,4-dichloronitropyrimidine, NaHCO$_3$, cHex, 16 h, 50 °C, 34−90%; (c) Fe, AcOH, 3−4 h, 70 °C, 25−42%; (d) MeI, NaH, DMF, 0 °C to rt, 16 h, 59−75%; (e) conc. HCl, EtOH/dioxane/H$_2$O, 1:1:1, 120 °C, 24−48 h, 7−53%; (f) H$_2$, 10% Pd·C, MeOH, rt, 1 h, 41−46%.

dual ALK−BRD inhibitor. In particular, we sought to reduce activity against PLK-1, improve ALK activity, and maintain BRD4 activity. To analyze the scope for modifications as well as derive design hypotheses, we first analyzed the published structures of BI-2536 bound to BRD4 and PLK-1.[14,21] In addition, we docked BI-2536 into ALK (2XB7) using Glide. We chose this structure for our docking experiment due to structural similarity between the ALK inhibitor NVP-TAE684[22] and BI-2536, in particular, the aminopyrimidine hinge binding motif and the *ortho*-methoxy phenyl group.

In BRD4, the methyl amide moiety acts as the acetylated lysine (KAc) mimetic, interacting with Asn140 (Figure 2a). As described in more detail previously,[14] additional interactions arise between the aminopyrimidine group and conserved waters in the ZA channel. The PLK-1-bound structure showed that the aminopyrimidine forms the key interactions with the hinge region of the kinase including Cys133 (Figure 2b). Docking into ALK not surprisingly predicted that amino-pyrimidine of BI-2536 interacted with the ALK hinge region including residue Met1199 in a manner similar to that for PLK-1 (Figure 2c). The amide carbonyl was also predicted to interact with conserved water in the back of the ALK pocket.

Based on the ALK docking and BRD4 X-ray structure, we wanted to maintain the key kinase and bromodomain binding motifs on the dihydropteridinone core and thus decided to leave these regions of the compound untouched.

Our analysis also suggested that several positions around the core structure offered significant scope for modification (Figure 2d). The first area chosen for modification was the (*R*)-ethyl group (R^1), which fits into a hydrophobic pocket in both PLK-1 and BRD4. The docking of BI-2536 in ALK also suggests that the (*R*)-ethyl is pointing toward a pocket formed by residues Val1130, Ala1148, Lys1150, and Leu1196. It has been reported that changing the chirality of the ethyl group has little effect on the potency at PLK-1 and BRD4, whereas removing the group afforded a 26-fold reduction in potency at BRD4.[24,25]

We were also interested in the cyclopentyl substitution off the dihydropteridinone core (R^2), which has been shown to be a region where BRD4 and PLK-1 selectivity can be tuned.[24] For example, changing the cyclopentyl to a 3-bromobenzyl group increases BRD4 affinity due to improved hydrophobic interactions with the WPF shelf but decreases PLK-1 activity, suggesting that modifications in this region could be used to improve selectivity against PLK-1.

Next, we considered the methoxy group at the R^3 position. Docking of BI-2536 suggests that the alkoxy group is pointing toward a known region for achieving ALK selectivity (Figure 2c).[21] The majority of kinases have a bulkier residue at this region, allowing ALK selectivity to be achieved as seen with ceritinib and alectinib.[26,27] In addition, larger alkoxy groups were known to improve interactions at BRD4.[24] We thus hypothesized that larger alkoxy groups will lead to increased selectivity against PLK-1 while maintaining BRD4 activity.

The final area chosen for modification is the solvent channel methylpiperidine group (R^4). Published structure−activity relationship (SAR) data for ALK inhibitors suggested that a wide variety of groups are tolerated in this region.[28−30] We particularly decided to prepare analogues without the amide group to reduce PLK-1 activity by removing a hydrogen-bonding interaction with Leu59 and a water molecule in the PLK-1 pocket.

Following this structure-based analysis and docking, we decided to focus modifications on four areas (R^1, R^2, R^3, and R^4) and to keep the dihydropteridinone core unchanged to maintain the key kinase and bromodomain binding inter-actions (Figure 2d).

Chemistry. We prepared a series of analogues of BI-2536 by adapting and optimizing previously described syntheses.[31] For aniline intermediates containing the R^3 and R^4 modifications, two routes were used as shown in Scheme 1. For the amide-containing intermediates, the isobutyl group was first introduced by alkylation to 3-hydroxy-4-nitrobenzoic acid **1** via protection and subsequent deprotection of the benzoic

Scheme 3
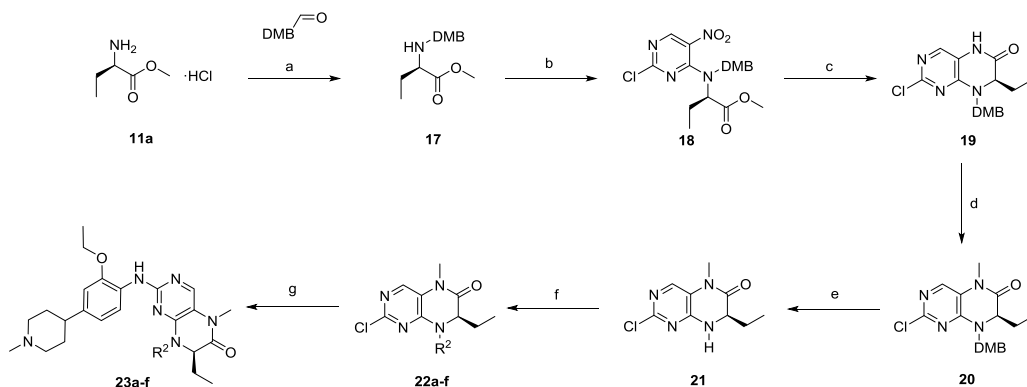
[a]Reagents and conditions: (a) NaBH(OAc)$_3$, NaOAc, DCE, rt, 16 h, 97%; (b) 2,4-dichloronitropyrimidine, NaHCO$_3$, cHex, 16 h, 50 °C, 78%; (c) H$_2$, PtO$_2$, VO(acac)$_2$, tetrahydrofuran (THF), 98%; (d) MeI, NaH, DMF, 0 °C to rt, 16 h, 86%; (e) TFA, 80 °C, 4 h, 66%; (f) R^2–X, NaH, DMF, rt, 16 h, 37–68%; (g) conc. HCl, EtOH/dioxane/H$_2$O, 1:1:1, 120 °C, 24–48 h, 9–32%.

acid. The 4-nitrobenzoic acid **3a** was coupled to 4-amino-1-methylpiperidine using O-(benzotriazol-1-yl)-N,N,N′,N′-tetra-methyluronium hexafluorophosphate (HBTU) to give amide **4a**, followed by reduction using SnCl$_2$ to give aniline **5a**. The ethoxy analogue **5b** was made via the same route from commercial compound **3b**. The synthesis of anilines **10a** and **10b** began with a Suzuki coupling between an alkoxy-nitrobenzene (**6a** and **6b**) and 4-pyridineboronic acid. Pyridines **7a** and **7b** were methylated to give **8a** and **8b** as the iodonium salts and then partially reduced using sodium borohydride (**9a** and **9b**). Hydrogenation of the dihydropyridine and nitro group gave aniline intermediates **10a** and **10b**.
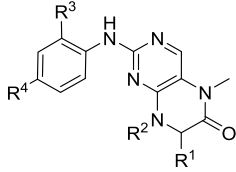
Meanwhile, intermediates **15a–g** were prepared according to Scheme 2. The appropriate amino acids **11a–c** underwent reductive amination with various aldehydes to give intermediates **12a–g** followed by regioselective S$_N$Ar with 2,5-dichloro-4-nitropyrimidine to give **13a–g**. Reductive hetero-cyclization using iron and acetic acid formed the dihydropter-idinone scaffold (**14a–g**), which was methylated to give intermediates **15a–g**. The final step was acid-promoted S$_N$Ar between intermediates **15a–g** and anilines **5a**, **5b**, **10a**, and **10b** to yield final compounds **16a–l**. Hydrogenation of compounds **16f** and **16h** to remove the bromine yielded compounds **16g** and **16i**.
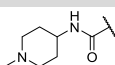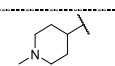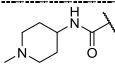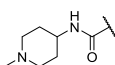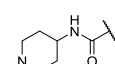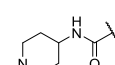
A key obstacle to preparing a significant number of analogues at the R^2 position was that this substituent was introduced early and preparation of each example required five steps (Scheme 2). To our surprise, there was no precedent for synthetic routes for late stage variation at this position. To facilitate preparation of these derivatives, we developed an alternative approach. This approach maintained many elements of the initial route (Scheme 3) but started with a dimethoxybenzyl (DMB) protecting group at the R^2 position. This strategy allowed us to remove the DMB group by refluxing the advanced intermediate (**20**) in trifluoroacetyl (TFA) and to subsequently introduce a wide range of R^2 groups. A key challenge was that the reductive cyclization step on intermediate **18** employing iron and acetic acid partially removed the DMB group. We tested a range of hydrogenation conditions and, gratifyingly, PtO$_2$ and VO(acac)$_2$ gave an excellent yield of 98%.[32] This route enabled us to prepare the key intermediate **21** on a multi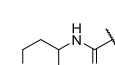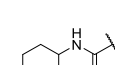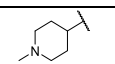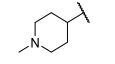gram scale and convert it into a range of final products (**23a–f**) in only two steps. Chiral shift NMR and chiral high-performance liquid chromatography

(HPLC) confirmed that no racemization took place under either the strongly basic or strongly acidic conditions. However, on a later repeat of this synthesis, we observed that epimerization could occur during the alkylation of **19** to yield **20**. Reanalysis of previous batches confirmed that no epimerization was observed in the synthesis of the batch used to prepare the compounds described in this article (Supp. Figure 1). Furthermore, we reanalyzed products of reactions obtained under similar alkylating conditions (Scheme 2), confirming that racemization had not occurred here either. All final products described here were thus unaffected by the epimerization. However, due to the potential for racemization, we sought to reoptimize this step. By reducing the number of equivalents of sodium hydride or replacing this with a weaker base such as sodium hydroxide, enantiomeric ratios of 9:1 or greater could be obtained.

Biological Testing. Table 1 shows the derivatives of BI-2536, modifying the R^1, R^2, R^3, and R^4 positions, and their activities at ALK^{F1174L}, BRD4, and PLK-1. The primary assays for biochemical testing were LanthaScreen for ALK^{F1174L} and thermal shift against BRD4 (10 μM compound concentration). For selected compounds, this was followed by isothermal calorimetry against BRD4 and/or a PLK-1 Z-Lyte assay.

We started by analyzing the effect of the amide functionality in the solvent channel group (R^4, Figure 2d). Removal of the amide group (compound **16a**) had little effect against ALK^{F1174L} and BRD4 potency. However, consistent with our hypothesis, it significantly decreased PLK-1-1 activity. Based on the measured IC$_{50}$ value of 2.6 nM, **16a** showed a four-fold reduction in potency against PLK-1. The real effect on PLK-1 potency of this structural change may be significantly greater, however, as the potency of BI-2536 is below the dynamic range of our assay. Next, we analyzed the effect of the R^3 substituent (Figure 2d) and prepared analogues with an ethoxy and an isobutoxy group at this position. The ethoxy group on compound **16c** gave a small reduction in potency against ALK^{F1174L} but a greater decrease in PLK-1 potency. An increase in the size of the group further to a butoxy group (compound **16b**) resulted in a much larger drop in potency against ALK^{F1174L}. For BRD4, increasing the group to ethoxy and isobutoxy gave only a small decrease in activity, confirming the tolerance of larger groups at this position. Compound **16c** provided the best balance of potency and selectivity thus far, so the ethoxy group was maintained.

Table 1. Structure−Activity Relationships of the R[1], R[2], R[3], and R[4] Groups

No.	R[1]	R[2]	R[3]	R[4]	ALK^{F1174L} IC$_{50}$ (nM)[a]	BRD4 T_m Shift (K)[b]	BRD4 K_d (nM)	PLK-1 IC$_{50}$ (nM)[a]
BI-2536	(R)-Et	cPe	OMe		180	5.7	37	< 2.6
16a	(R)-Et	cPe	OMe		290	5.4	80	9.9
16b	(R)-Et	cPe	OiBu		1700	7.2	73	43% at 10 nM
16c	(R)-Et	cPe	OEt		380	6.0	81	12
16d	(S)-Et	cPe	OEt		3400	-0.2	n.d	19% at 10nM
16e	H	cPe	OEt		520	0.2	n.d	32% at 10 nM
16f	(R)-Et	3-BrBn	OEt		490	6.7	73	110
16g	(R)-Et	Bn	OEt		440	4.1	69	84
16h	(R)-Et	3-BrBn	OEt		290	5.0	120	540
16i	(R)-Et	Bn	OEt		85	4.7	54	290

[a]Data represents the geometric mean; see Supp. Table 1 for full statistics. n.d. = not determined. [b]T_m shift determined at compound concentration of 10 μM, n = 2.

We started testing the effect of the R[1] group by removing the (R)-ethyl group (16e). This removal reduced potency at BRD4 and PLK-1 very likely due to the loss of favorable interactions with the aforementioned pockets in BRD4 and PLK-1. Similarly, removal of the (R)-Et group also reduced ALK^{F1174L} potency 3-fold. We also synthesized the opposite enantiomer 16d, which also significantly reduced potency at all three targets. The reduction in PLK-1 and BRD4 activity was not in agreement with a published study but consistent with loss of productive interactions of the (R)-Et group with both PLK-1 and BRD4 and supported by modeling, which suggests that the ethyl group is too big to be accommodated on the lower face of the PLK-1 pocket. Finally, we analyzed substitution at the R[2] position. Compounds 16f and 16g

with a 3-bromobenzyl and benzyl group, respectively, maintained BRD4 activity and led to a 30−40-fold decrease of the PLK-1 activity, as expected from previous reports.[24] Compounds 16f and 16g were equipotent in ALK^{F1174L} activity, compared with 16c. Importantly, the divergent SAR between ALK and PLK-1 with 16f and 16g supported our hypothesis that it is possible to optimize the ALK/PLK-1 selectivity window at the R[2] position.

To conclude this initial SAR investigation, we combined modifications that showed a decrease in PLK-1 potency. Compounds 16h and 16i with the combined modifications of the benzyl or 3-bromobenzyl group at R[2], ethoxy group at R[3], and removal of the amide at R[4] gave a greater decrease in PLK-1 activity (>100−200-fold). With benzyl compound 16i, we
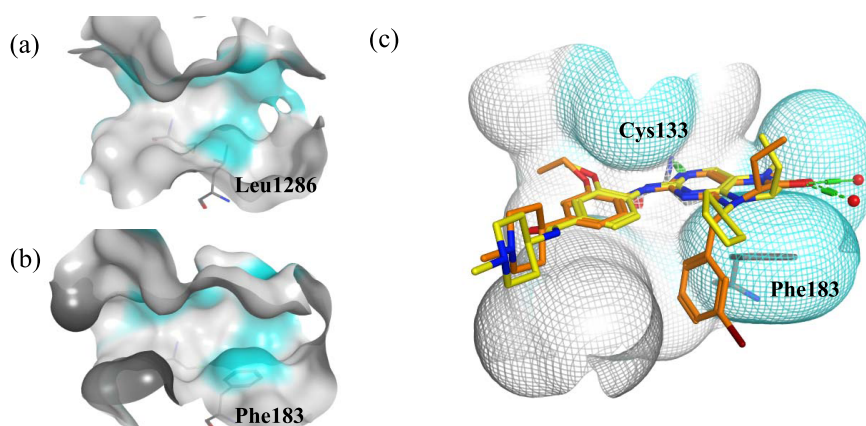
Figure 3. Surfaces of (a) ALK (2XB7) and (b) PLK-1 (2RKU) highlighting residues Leu1256 and Phe183. (c) Docking pose generated using Glide showing **16h** (orange) in complex with PLK-1 (2RKU), overlaid with X-ray structure of BI-2536 (yellow) in PLK-1 (2RKU).

also saw a 2-fold increase in ALK^{F1174L} potency and maintained potent BRD4 activity. This was the first analogue demonstrating greater potency at ALK^{F1174L} than at PLK-1.

R^2 SAR. So far, the greatest change in PLK-1 activity resulted from modifying the cyclopentyl to a benzyl or 3-bromobenzyl group (Table 1). Further inspection of this region in ALK and PLK-1 structures shows that PLK-1 has a larger phenylalanine residue (Phe183) at the bottom of this pocket compared with a smaller leucine residue (Leu1286) in ALK (Figure 3a,b). We hypothesized that PLK-1 inhibition would be less tolerant to substitution at the R^2 position due to this geometric constraint compared to that in the more open ALK structure. To investigate this hypothesis further, we performed docking studies of 3-bromobenzyl analogue **16h** in PLK-1 (Figure 3c). The aminopyrimidine moiety was still predicted to bind to the hinge region including Cys133, but a shift in the core was observed. Additionally, the core of the molecule adopts a more strained, puckered conformation. Both differences from the observed binding mode were likely caused by clashes of the bromobenzyl group with the side chain of Phe183 and were consistent with the decrease in activity observed with benzyl analogues **16f**−**i**. We thus decided to explore if this key amino acid difference can be exploited to discover compounds with improved ALK potency and PLK-1 selectivity.

To enable structure-based design, we attempted to solve cocrystal structures of our compounds bound to ALK. However, these attempts failed, likely due to the still modest activity. Due to the lack of structural information, we decided to probe the ALK pocket through systematic synthesis and testing.

Using the modified route in Scheme 3 to facilitate preparation of analogues at the R^2 position, we prepared compounds **23a**−**c** to analyze the effect of different substitutions at the 3-benzyl position. While these compounds maintained the BRD4 activity, we did not observe improvements in ALK^{F1174L} potency or PLK-1 selectivity, aside from compound **23b** that contains a 3-cyanobenzyl group. The PLK-1 IC$_{50}$ was 1.8 μM, a >700-fold decrease from starting compound BI-2536, leading to an improved (5-fold) ALK selectivity over PLK-1. Compound **23b** demonstrated that PLK-1 activity can be substantially reduced by varying this position, but we were still yet to find a group that achieved this while maintaining or improving ALK^{F1174L} potency. Next, we considered changing the substitution position on the benzyl
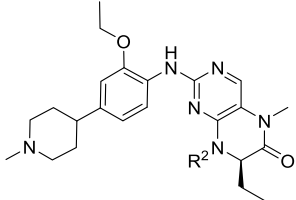
ring. However, the *ortho*- and *para*-bromobenzyls **23d** and **23e** showed no improvement in ALK^{F1174L} potency compared with meta-analogue **16h** and were still not as potent as unsubstituted benzyl analogue **16i**.
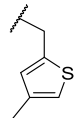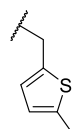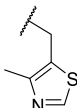
We then considered heterocycle substituents. Thiazole **23f** showed a decrease in ALK^{F1174L} activity, but exploring thiophenes proved to be more productive. Compound **16j** gave encouraging IC$_{50}$s against ALK^{F1174L} and BRD4, yet the ALK/PLK ratio dropped to 1:1. Following from this result, we moved the methyl group around the thiophene ring. Derivative **16k** with the methyl group at the 4-position showed potent inhibition of ALK^{F1174L} (IC$_{50}$ = 17 nM) and through this gain in potency also a 7-fold selectivity window over PLK-1. Gratifyingly, the compound retained BRD4 activity (Table 2).

We next determined the cocrystal structures of **16i** and **16k** with BRD4 (Figure 4 and Supp. Table 3). The compounds bound into the acetyllysine-binding site with the methyl amide moiety retaining the key hydrogen bond interaction with asparagine N140. The methyl amide and pyrimidine moieties in both compounds retain interactions with conserved waters in the BRD4 pocket, whereas the thiophene and benzyl R^2 substituents are situated in the hydrophobic WPF shelf region.

With compound **16k**, we had a compound in hand that showed satisfactory IC$_{50}$s against ALK^{F1174L} and BRD4 and a selectivity window over PLK-1. We decided to profile **16k** further by examining the physicochemical properties and broader kinase and bromodomain selectivity. Lipophilicity was measured using the SiriusT3 potentiometric method, giving a high log P of 6.1 (Table 3). It is notable that the measured log $D_{7.4}$ of 4.2 is significantly lower due to protonation of the piperidine basic center, which can also account for the good solubility. In addition, the compound shows good permeability as measured in a PAMPA permeability assay.

Next, we considered the broader kinase and bromodomain selectivity of **16k** to assess if the compound maintained the selectivity across both protein families. Compound **16k** was first tested against a panel of BET and non-BET bromodomains. In this panel, **16k** exhibited excellent BET family selectivity, in common with BI-2536 and other BET inhibitors (Figure 5a and Supp. Table 4).[14,33,34] We then tested **16k** against the DiscoverX *scan*EDGE panel of 97 kinases at a single point concentration of 1 μM.[35] Gratifyingly, only four kinases were identified as hits, confirming that we had maintained broad kinome selectivity; the greatest inhibition was observed for ALK wild type (WT) and PLK-1

Table 2. Structure−Activity Relationships of the R² Group[c]

No.	R²	ALK[F1174L] IC_{50} (nM)[a]	BRD4 T_m Shift (K)[a,b]	BRD4 K_d (nM)	PLK-1 IC_{50} (nM)[a]
16i	Bn	85	4.7	54	290
16h	3-BrBn	290	5.0	120	540
23a	3-ClBn	210	6.2	130	540
23b	3-CNBn	370	4.8	78	1800
23c	3-OMeBn	350	5.1	n.d	n.d
23d	2-BrBn	150	2.9	n.d	n.d
23e	4-BrBn	680	5.8	n.d	n.d
16j[b]	(3-methylthiophen-2-ylmethyl)	63	5.4	63	68
16k[b]	(4-methylthiophen-2-ylmethyl)	17	7.1	44	125
16l[b]	(5-methylthiophen-2-ylmethyl)	220	8.3	n.d	n.d
23f	(4-methylthiazol-5-ylmethyl)	370	4.6	n.d	n.d

[a]Data represents the geometric mean; see Supp. Table 2 for full statistics. n.d. = not determined. [b]Final compounds synthesized using Scheme 2. [c]T_m shift determined at compound concentration of 10 μM, $n = 2$.
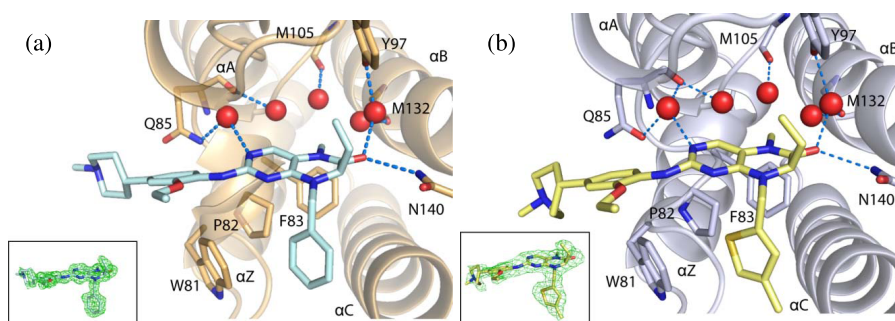
Figure 4. (a) Cocrystal structure of **16i** with BRD4 (6Q3Y) and associated $|2F_O| − |F_C|$ refined electron density map contoured at 1σ. (b) Cocrystal structure of **16k** with BRD4 (6Q3Z) and associated $|2F_O| − |F_C|$ refined electron density map contoured at 1σ.

followed by insulin receptor (INSR) and PLK-3 (Figure 5b and Table 4). We attributed the observed broad kinase selectivity of **16k** at least partially to be due to the ethoxy group.[21,27] This was based on the observation that the kinases that showed significant inhibition (ALK, PLK-1, PLK-3, and INSR) indeed feature a smaller leucine residue in the hinge

H

Table 3. Physicochemical Properties of 16k

parameter	result
solubility (HPLC)[a]	90 μM
PAMPA pH$_{7.4}$	49×10^{-6} cm/s
log P	6.1
log $D_{7.4}$	4.2

[a]Solubility measured via an in-house HPLC method from phosphate buffer at pH 7.4.

Table 4. K_ds of 16k against the Kinase Screening Hits

kinase	hits at 1 μM (% control)	K_d (nM)
ALK WT	7.1	89
INSR	25	190
PLK-1	1	11
PLK-3	25	160
ALK^{F1174L}		23

region that can accommodate the ethoxy group (Supp. Table 5).
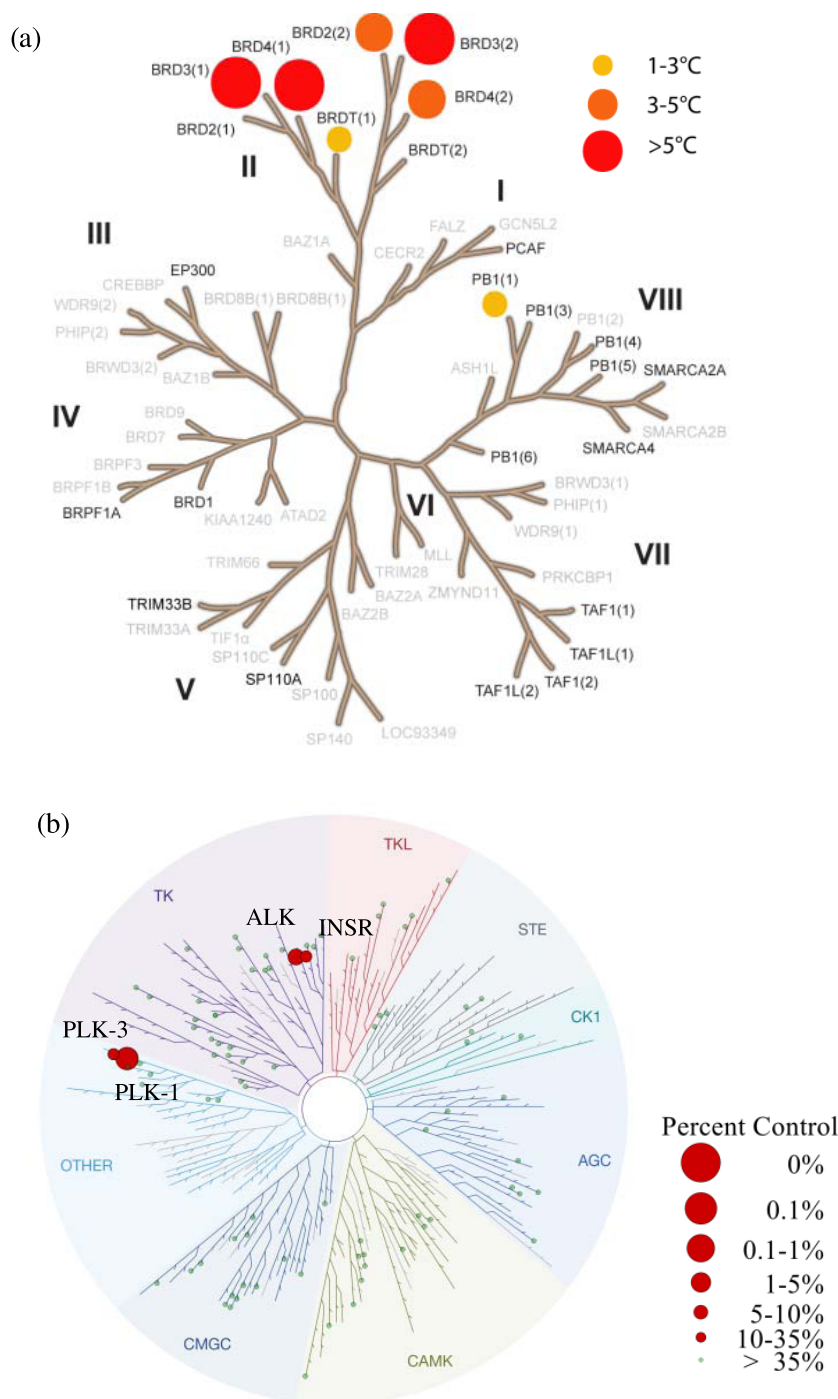
Figure 5. (a) Screening of **16k** against a panel of 25 bromodomains, showing ΔT_m as circles. Larger circles indicate greater ΔT_m. (b) Screening of **16k** against the DiscoverX *scan*EDGE panel of 97 kinases at a single point concentration of 1 μM. Larger circles indicate a stronger hit.

Compound	IC$_{50}$
BI-2536	> 9.4 μM
16k	1.5 μM
Ceritinib	79 nM

Figure 6. ALK MSD immunoassay measuring ALK phosphorylation in the Kelly cell line. The plot shows the ratio of phosphorylated ALK to total ALK.

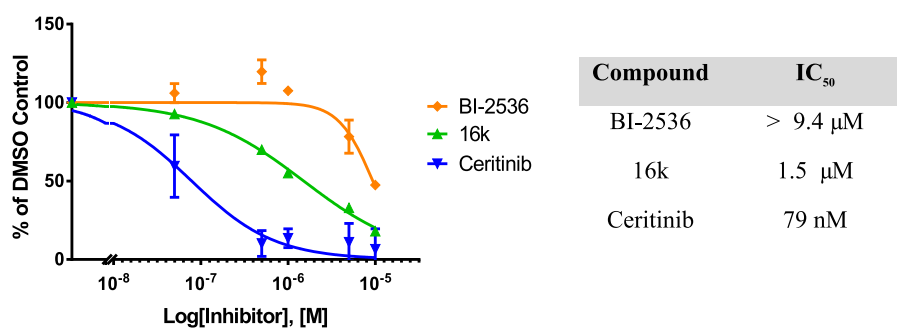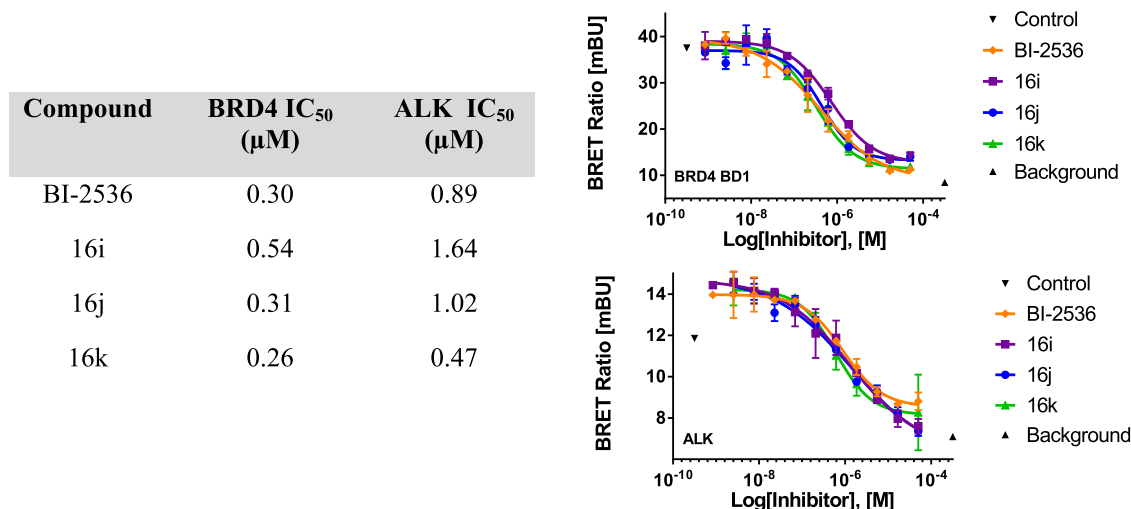| Compound	BRD4 IC$_{50}$ (μM)	ALK IC$_{50}$ (μM)
BI-2536	0.30	0.89
16i	0.54	1.64
16j	0.31	1.02
16k	0.26	0.47

Figure 7. NanoBRET data for lead compounds **16i–k** against ALK and BRD4 in HEK293T cells.

Demonstrating Target Engagement in Cells. We next tested our lead compounds in the cellular context to confirm that we had on-target engagement of ALK and BRD4 in cells. We first tested the effect of compound **16k** on autophosphorylation of the ALK^{F1174L} mutant in Kelly neuroblastoma cells using an meso-scale discovery (MSD) assay (Figure 6). For comparison, we also tested our starting point BI-2536 and the Food and Drug Administration-approved ALK inhibitor ceritinib[26] as a positive control. Compound **16k** showed inhibition of ALK^{F1174L} phosphorylation levels, in line with what was expected from the biochemical IC$_{50}$ and representing a significant improvement from starting compound BI-2536.

We also measured the cellular potency of our lead compounds against BRD4 and ALK WT using NanoBRET assays (Figure 7 and Supp. Table 6). Compound **16k** showed a cellular potency of 470 nM against ALK WT and 260 nM against BRD4. The BRD4 cellular potency was comparable to that of starting compound BI-2536, consistent with the compound's minimal disruption to the key interactions with the BRD4 pocket. The results of the ALK autophosphorylation assay and NanoBRET experiments demonstrated that **16k** inhibited both ALK^{F1174L} and BRD4 in cells.

Cellular Kinase Selectivity. The observation that the biochemical potency of **16k** translated efficiently into cellular assays with a relatively minor drop-off consistent with other ALK inhibitors prompted us to investigate the selectivity against PLK-1 in cells. Despite very good overall selectivity in the DiscoverX scan, **16k** showed similar K_ds for the ALK^{F1174L} mutant and PLK-1 (23 vs 11 nM, Table 4). However, given

the small cellular drop-off for ALK mentioned above, we speculated that a larger drop-off for PLK-1 may lead to a better selectivity window. To investigate this hypothesis, we investigated markers of PLK-1 inhibition in cells, namely, mitotic arrest in the G2/M phase and increased concentrations of PLK-1, cyclin B1, and phosphohistone H3. Indeed, BI-2536 has been published to show effects on these markers at concentration around 50 nM, which is a 250-fold drop-off from its K_d of 0.19 nM.[36] As compound **16k** is structurally similar to BI-2536, we would expect to see a similar potency drop-off in cells, in this case to >2.5 μM. To assess the cellular selectivity, we assessed the effect of compounds **16k** and BI-2536 on HeLa cells. Consistent with data mentioned above, BI-2536 induced mitotic arrest and increased concentrations of PLK-1, cyclin B1, and phosphohistone H3 at a concentration as low as 50 nM (Figure 8).[36] In addition, we observed an increase in PLK-1 phosphorylation at sites T210 and S137. In strong contrast, compound **16k** did not cause an increase in levels of these mitotic markers and phosphorylation sites up to concentrations of 10 μM and thus well beyond the concentration where ALK^{F1174L} and BRD4 are inhibited in the cellular context. Quantitative analysis of the cell cycle distribution by flow cytometry supported the data obtained by Western blot analysis (Supp. Figure 2).

Based on the cellular data, the combination of the reduction in PLK-1 activity and the improvement in ALK^{F1174L} activity thus resulted in a >10−20-fold selectivity window for ALK^{F1174L} over PLK-1 in cells. Compound **16k** thus
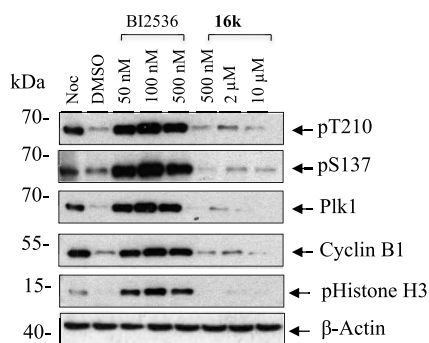
J

Figure 8. Induction of mitotic arrest by BI-2536 and **16k** in HeLa cells. Changes in the fraction of cells arrested in mitosis were analyzed by Western blots against phosphorylation sites pT210 and pS137 and mitotic markers PLK-1, cyclin B1, and phosphohistone H3.

represented a significant step toward discovering drugs that concomitantly target mutant ALK and BRD4.

CONCLUSIONS

To our knowledge, we report the first combined ALK−BRD4 inhibitor (**16k**). Moreover, our work is one of the few examples where medicinal chemistry design was applied to combine inhibition of a specific kinase (in this case ALK) with BRD4 inhibition to discover a dual inhibitor for a clearly defined therapeutic hypothesis.

We started from the known dual inhibitor BI-2536 that inhibits PLK-1 and BRD4. Interestingly, although tuning the PLK-1 and BRD4 activity of BI-2536 has been disclosed, changing the kinase activity to another target and hence to a new dual kinase−bromodomain combination has not been reported.[24,25] Exploring a structure-based design, we discovered compounds with significantly improved ALK activity and greatly reduced PLK-1 activity while maintaining BRD4 potency and overall kinome selectivity. Our lead compound demonstrates on-target engagement of ALK and BRD4 in cellular assays and favorable broad kinase and bromodomain selectivity. In particular, the compound showed selectivity over PLK-1 in cells underlining the design effort to change the kinase selectivity from PLK-1 to ALK.

Our work also highlighted the well-known challenges of designing and discovering dual inhibitors that inhibit two, structurally distinct proteins. A particular challenge is to incorporate two distinct pharmacophores that ensure not only potent inhibition of both targets but also selectivity within these protein families (in our case, kinases and bromodomains) into one druglike compound.

Despite these challenges, we achieved significant steps toward a dual ALK and BRD4 inhibitor. Key to this progress was choosing a starting point that contained an alkoxy group that is tolerated only by a few kinases including ALK and PLK-1. By maintaining this throughout, we achieved a compound with satisfactory overall kinome selectivity.

Our main optimization goal starting from BI-2536 was to significantly improve ALK activity and PLK-1 selectivity. The challenge here was that key regions of BI-2536 had to remain untouched to maintain the BRD4 activity. In particular, the methyl substituent that points toward the gatekeeper and the ethyl group would have been promising places to improve activity for ALK and selectivity over PLK-1. However, both moieties are essential for potent binding to BRD4 and could

hence not be changed. Crucially, our structure-based analysis also suggested that the R^2 substituent can be modified without losing BRD4 activity and that optimizing this part of the molecule was a promising approach to achieve our goal of shifting kinase selectivity, as exemplified by **16k**.

We thus conclude that, not surprisingly, the quality and properties of the selected starting point matter even more for programs aiming at dual inhibitors since the options for chemical optimization will be significantly more limited. Directly related to that, the challenge of discovering dual inhibitors is somewhat less daunting when both targets tolerated a range of different chemotypes and inhibitors, thus increasing the chance that a starting point with already favorable properties can be explored.

EXPERIMENTAL SECTION

General Synthetic Information. All anhydrous solvents and reagents were obtained from commercial suppliers and used without further purification. All reactions were carried out under a positive pressure of N_2, and moisture-sensitive reagents were transferred via a syringe. Evaporation of solvent was carried out using a rotary evaporator under reduced pressure at a bath temperature of up to 60 °C. Column chromatography was carried out using a Biotage SP4 purification system using Biotage SNAP Kp-Si cartridges. Semi-preparative separations were carried out using a 1200 series preparative HPLC over a 15 min gradient elution (Grad15-min20mls.m) from 90:10 to 0:100 water/methanol (both modified with 0.1% formic acid) at a flow rate of 20 mL/min. Microwave-assisted reactions were carried out using a Biotage Initiator microwave system. In general, the course of reactions was followed by thin layer chromatography or mass spectroscopy. All final compounds were purified to ≥95% purity.

NMR spectra were recorded on a Bruker AMX 500 (500 MHz) spectrometer using a deutrated solvent. NMR data is presented in the form of chemical shift δ (multiplicity, coupling constants, and integration) for major diagnostic protons, given in parts per million (ppm) relative to tetramethylsilane as an internal standard. High-resolution mass spectrometry (HRMS) was assessed using an Agilent 1200 series HPL and diode array detector coupled to a 6120 time-of-flight mass spectrometer with a dual multimode atmospheric-pressure chemical ionization/electrospray ionization (ESI) source. Analytical separation was carried out at 30 °C on a Merck Purospher STAR column (RP-18e, 30 × 4 mm^2) using a flow rate of 1.5 mL/min in a 4 min gradient elution; solvents: aqueous (0.1% formic aid) and methanol, monitored at a wavelength of 254 nm. Optical rotation was determined by an ADP 440 polarimeter. Specific rotations $[\alpha]_D$ are given in deg cm^3/(g dm).

Methyl 3-Isobutoxy-4-nitrobenzoate (2). Step 1: 3-Hydroxy-4-nitrobenzoic acid **1** (500 mg, 2.73 mmol) was suspended in MeOH (0.1 M), and SOCl$_2$ (0.40 mL, 5.46 mmol) was added slowly at 0 °C. The reaction was heated at reflux for 4 h. Upon completion, the volatiles were removed in vacuo and the residue was triturated with diethyl ether. The resulting solid was filtered and dried under vacuum to afford methyl 3-hydroxy-4-nitrobenzoate (HCl salt) as a yellow solid (576 mg, 90%). δ_H (500 MHz, CDCl$_3$): 10.51 (s, 1H), 8.18 (d, J = 8.5 Hz, 1H), 7.84 (d, J = 1.6 Hz, 1H), 7.62 (dd, J = 8.5, 1.6 Hz, 1H), 3.97 (s, 3H). Step 2: To the crude product in DMF (0.1 M) was added K$_2$CO$_3$ (592 mg, 4.28 mmol) and 1-iodo-2-methylpropane (142 μL, 1.20 mmol), and the reaction was stirred at 50 °C for 16 h. Upon completion, EtOAc was added and the mixture was washed with water (×2) and brine (×1), dried over MgSO4, filtered, and concentrated in vacuo. The residue was purified by Biotage column chromatography (cHex/EtOAc, 0−20%) to afford **2** as a colorless oil (158 mg, 0.62 mmol 73%). δ_H (500 MHz, CDCl$_3$): 7.81 (d, J = 8.2 Hz, 1H), 7.71 (d, J = 1.6 Hz, 1H), 7.67−7.64 (m, 1H), 3.96 (s, 3H), 3.92 (d, J = 6.3 Hz, 1H), 2.20−2.11 (m, 1H), 1.05 (d, J = 6.9 Hz, 6H).

3-Isobutoxy-4-nitrobenzoic Acid (3a). To **2** (150 mg, 0.59 mmol) in a solvent mixture of THF/H_2O (1:1, 0.1 M) was added LiOH (142 mg, 5.92 mmol), and the reaction was stirred for 18 h. Upon completion, the aqueous layer was acidified with 1 M HCl until pH 1 was reached and extracted with EtOAc (×3). The combined organic phases were dried over $MgSO_4$, filtered, and concentrated in vacuo to afford **3a** as a yellow solid (100 mg, 0.42 mmol, 71%). δ_H (500 MHz, $CDCl_3$): 7.85 (d, J = 8.2 Hz, 1H), 7.79 (d, J = 1.3 Hz, 1H), 7.76 (dd, J = 8.2, 1.3 Hz, 1H), 3.95 (d, J = 6.3 Hz, 1H), 2.23−2.14 (m, 1H), 1.08 (d, J = 6.9 Hz, 6H).

3-Isobutoxy-N-(1-methylpiperidin-4-yl)-4-nitrobenzamide (4a). To a solution of **3a** (50 mg, 0.21 mmol) in DMF (0.1 M) was added HBTU (127 mg, 0.33 mmol), Et_3N (58 μL, 0.41 mmol), and 1-methylpiperidin-4-amine (23.9 mg, 0.21 mmol), and the reaction was stirred for 18 h. Upon completion, the reaction mixture was partitioned between EtOAc and water and the aqueous layer was extracted with EtOAc (×2). The organic phases were combined, dried over $MgSO_4$, filtered, and concentrated in vacuo. The residue was purified by Biotage column chromatography (dichloromethane (DCM)/MeOH, 0−10%) to afford **4a** as a yellow solid (60 mg, 0.18 mmol, 86%). HRMS (ESI +ve): found $[M]^+$ 336.1927, $[C_{17}H_{24}N_3O_4]^+$ requires 336.1923; δ_H (500 MHz, $CDCl_3$) 7.81 (d, J = 8.2 Hz, 1H), 7.55 (d, J = 1.6 Hz, 1H), 7.28 (dd, J = 8.2, 1.6 Hz, 1H), 6.44 (d, J = 7.6 Hz, 1H), 4.06−3.97 (m, 1H), 3.92 (d, J = 6.3 Hz, 2H), 2.94 (d, J = 11.7 Hz, 2H), 2.37 (s, 3H), 2.30−2.25 (m, 2H), 2.18−2.10 (m, 1H), 2.09−2.03 (m, 2H), 1.78−1.69 (m, 2H), 1.04 (d, J = 6.6 Hz, 6H).

3-Ethoxy-N-(1-methylpiperidin-4-yl)-4-nitrobenzamide (4b). **4b** was synthesized in 77% yield (orange solid, 111 mg, 0.36 mmol) according to the same procedure as **4a**, from **3b** (100 mg, 0.47 mmol) and 1-methylpiperidin-4-amine (54.1 mg, 0.47 mmol). HRMS (ESI +ve): found $[M]^+$ 308.1624 $[C_{15}H_{21}N_3O_4]^+$ requires 308.1610; δ_H (500 MHz, $CDCl_3$): 7.82 (d, J = 8.2 Hz, 1H), 7.58 (d, J = 1.9 Hz, 1H), 7.23 (dd, J = 8.2, 1.9 Hz, 1H), 5.99 (d, J = 7.3 Hz, 1H), 4.26 (q, J = 7.2 Hz, 2H), 4.05−3.94 (m, 1H), 2.87 (d, J = 11.2 Hz, 2H), 2.33 (s, 3H), 2.19 (t, J = 11.2 Hz, 2H), 2.10−2.03 (m, 2H), 1.65−1.56 (m, 2H), 1.49 (t, J = 6.9 Hz, 3H).

4-Amino-3-isobutoxy-N-(1-methylpiperidin-4-yl)benzamide (5a). **4a** (60 mg, 0.18 mmol) was dissolved in a solvent mixture of EtOAc/EtOH (10:3, 0.1 M) to which tin(II) chloride dihydrate (202 mg, 0.89 mmol) was added. The reaction was stirred for 16 h at 50 °C. Upon completion, $NaHCO_3$ was added and the aqueous layer was extracted with EtOAc (×3). The combined organic phases were dried over $MgSO_4$, filtered, and concentrated in vacuo to afford **5a** as a yellow solid (30 mg, 99 μmol, 55%). HRMS (ESI +ve): found $[M]^+$ 306.22161, $[C_{17}H_{28}N_3O_2]^+$ requires 306.2176; δ_H (500 MHz, $CDCl_3$) 7.32 (d, J = 1.9 Hz, 1H), 7.10 (d, J = 8.2, 1.9 Hz, 1H), 6.66 (d, J = 8.2 Hz, 1H), 5.86 (d, J = 6.3 Hz, 1H), 4.12 (s, 2H), 4.02−3.92 (m, 1H), 3.83 (d, J = 6.3 Hz, 2H), 2.83 (d, J = 11.0 Hz, 2H), 2.31 (s, 3H), 2.22−2.09 (m, 3H), 2.07−2.00 (m, 2H), 1.57 (qd, J = 11.7, 3.6 Hz, 2H), 1.04 (d, J = 6.9 Hz, 6H).

4-Amino-3-ethoxy-N-(1-methylpiperidin-4-yl)benzamide (5b). **5b** was synthesized in 53% yield (yellow solid, 46 mg, 0.16 mmol) according to the same procedure as **5a**, from **4b** (95 mg, 0.31 mmol). HRMS (ESI +ve): found $[M]^+$ 278.1874 $[C_{15}H_{23}N_3O_2]^+$ requires 278.1863; δ_H (500 MHz, $CDCl_3$) 7.33 (d, J = 1.9 Hz, 1H), 7.11 (dd, J = 8.1, 1.9 Hz, 1H), 6.66 (d, J = 8.1 Hz, 1H), 5.86 (d, J = 7.3 Hz, 1H), 4.18−4.09 (m, 4H), 4.05−3.94 (m, 1H), 2.86 (d, J = 11.0 Hz, 2H), 2.33 (s, 3H), 2.23−2.18 (m, 2H), 2.04 (d, J = 10.4 Hz, 2H), 1.61−1.57 (m, 2H), 1.45 (t, J = 6.9 Hz, 3H).

4-(3-Ethoxy-4-nitrophenyl)pyridine (7a). 4-Bromo-2-ethoxy-1-nitrobenzene **6a** (1.5 g, 6.10 mmol), pyridine-4-ylboronic acid (749 mg, 6.10 mmol), Na_2CO_3 (1.1 g, 10.0 mmol), and $Pd(PPh_3)_2Cl_2$ (160 mg, 0.23 mmol) were dissolved in a solvent mixture of dioxane/water (6:1, 0.38 M) and heated at 110 °C for 45 min under microwave irradiation. Upon completion, the mixture was partitioned between EtOAc and water and the aqueous phase was extracted with EtOAc (×2) and DCM (×1). The organic phases were combined, dried over $MgSO_4$, filtered, and concentrated in vacuo. The residue was purified by Biotage column chromatography (DCM/MeOH, 9:1) to afford **7a**

as a yellow solid (81 mg, 3.32 mmol, 54%). HRMS (ESI +ve): found $[M]^+$ 245.0917 $[C_{13}H_{12}N_2O_3]^+$ requires 245.0921; δ_H (500 MHz, $CDCl_3$): 8.74 (dd, J = 4.4, 1.19 Hz, 2H), 7.96 (d, J = 8.5 Hz, 1H), 7.49 (d, J = 4.4, 1.6 Hz, 2H), 7.27−7.24 (m, 2H), 4.28 (q, J = 7.0 Hz, 2H), 1.53 (dt, J = 7.0 Hz, 3H)

4-(3-Methoxy-4-nitrophenyl)pyridine (7b). **7b** was synthesized in 65% yield (yellow solid, 200 mg, 0.87 mmol) according to the same procedure as **7a**, from 4-chloro-2-methoxy-1-nitrobenzene **6b** (250 g, 1.33 mmol) and pyridine-4-ylboronic acid (164 mg, 1.33 mmol). HRMS (ESI +ve): found $[M]^+$ 231.0803 $[C_{12}H_{10}N_2O_3]^+$ requires 231.0770; δ_H (500 MHz, $CDCl_3$): 8.74−8.72 (dd, J = 4.4, 1.6 Hz, 2H), 7.99 (dd, J = 8.8 Hz, 1H), 7.51 (dd, J = 4.4, 1.6 Hz, 2H), 7.28−7.25 (m, 2H), 4.05 (s, 3H).

4-(3-Ethoxy-4-nitrophenyl)-1-methylpyridin1-ium Iodide (8a). **7a** (600 mg, 2.47 mmol) and methyl iodide (0.54 mL, 8.65 mmol) were dissolved in acetonitrile (0.1 M), and the reaction was heated for 4 h at 50 °C. Upon completion, the mixture was concentrated in vacuo to afford **8a** as a yellow solid (945 mg, 2.45 mmol, 99%). HRMS (ESI +ve): found $[M]^+$ 259.1076 $[C_{14}H_{15}N_2O_3]^+$ requires 259.1082; δ_H (500 MHz, $MeOD_4$) 8.99 (d, J = 6.7 Hz, 2H), 8.48 (d, J = 6.7 Hz, 2H), 7.99 (d, J = 8.5 Hz, 1H), 7.79 (d, J = 1.8 Hz, 1H), 7.65 (dd, J = 8.5, 1.8 Hz, 1H), 4.46 (s, 3H), 4.38 (q, J = 6.9 Hz, 2H), 1.49 (t, J = 6.9 Hz, 3H).

4-(3-Methoxy-4-nitrophenyl)-1-methylpyridin1-ium Iodide (8b). **8b** was synthesized in 91% yield (yellow solid, 295 mg, 0.79 mmol) according to the same procedure as **8a**, from **7b** (200 mg, 0.87 mmol) and methyl iodide (0.19 mL, 3.04 mmol). HRMS (ESI +ve): found $[M]^+$ 245.0920 $[C_{13}H_{13}N_2O_3]^+$ requires 245.0926; δ_H (500 MHz, $MeOD_4$) 8.99 (d, J = 6.7 Hz, 2H), 8.49 (d, J = 6.7 Hz, 2H), 8.01 (d, J = 8.2 Hz, 1H), 7.81 (d, J = 1.9 Hz, 1H), 7.66 (dd, J = 8.2, 1.9 Hz, 1H), 4.45 (s, 3H), 4.10 (s, 3H).

4-(3-Ethoxy-4-nitrophenyl)-1-methyl-1,2,3,6-tetrahydropyridine (9a). **8a** (945 mg, 2.45 mmol) was dissolved in MeOH (0.05 M) and cooled to 0 °C. $NaBH_4$ (943 mg, 24.5 mmol) was slowly added in batches, and the reaction was stirred at rt for 2 h. The reaction was quenched with 1 M HCl, and MeOH was partially removed in vacuo. The residue was partitioned between EtOAc and 1 M NaOH until pH 12 was reached. The EtOAc layer was washed with 1 M NaOH, dried over $MgSO_4$, filtered, and concentrated in vacuo to give **9a** as a yellow oil (609 mg, 2.32 mmol, 95%). HRMS (ESI +ve): found $[M]^+$ 263.1387 $[C_{14}H_{18}N_2O_3]^+$ requires 263.1390; δ_H (500 MHz, $CDCl_3$): 7.85 (d, J = 8.5 Hz, 1H), 7.04−7.00 (m, 2H), 6.21−6.18 (m, 1H), 4.20 (q, J = 6.9 Hz, 2H), 3.17−3.14 (m, 2H), 2.69 (t, J = 5.7 Hz, 2H), 2.60−2.56 (m, 2H), 2.43 (s, 3H), 1.49 (t, J = 6.9 Hz, 3H).

4-(3-Methoxy-4-nitrophenyl)-1-methyl-1,2,3,6-tetrahydropyridine (9b). **9b** was synthesized in 56% yield (yellow oil, 80 mg, 0.32 mmol) according to the same procedure as **9a**, from **8b** (212 mg, 0.57 mmol). HRMS (ESI +ve): found $[M]^+$ 245.1239 $[C_{13}H_{13}N_2O_3]^+$ requires 249.1243; δ_H (500 MHz, $CDCl_3$): 7.85 (d, J = 8.5 Hz, 1H), 7.04 (d, J = 1.9 Hz, 1H), 7.02 (dd, J = 8.5, 1.9 Hz, 1H), 6.20 (tt, J = 3.5, 1.6 Hz, 1H), 3.96 (s, 3H), 3.16 (d, J = 2.85 Hz, 2H), 2.71−2.67 (m, 2H), 2.60−2.56 (m, 2H), 2.42 (s, 3H).

2-Ethoxy-4-(1-methylpiperidin-4-yl)aniline (10a). **9a** (600 mg, 2.32 mmol) and PtO_2 (158 mg, 0.70 mmol) were dissolved in acetic acid (0.03 M), and the mixture was purged with N_2. The mixture was placed under 50 psi of H_2 gas at rt for 16 h. The mixture was filtered through celite, washed with MeOH, and concentrated in vacuo. The residue was purified by Biotage column chromatography (DCM/MeOH, 9:1) to afford **10a** as an orange oil (410 mg, 1.75 mmol, 75%). HRMS (ESI +ve): found $[M]^+$ 235.1819 $[C_{14}H_{22}N_2O]^+$ requires 235.1809; δ_H (500 MHz, $CDCl_3$) 6.68−6.60 (m, 3H), 4.05 (q, J = 7.0 Hz, 2H), 3.20 (d, J = 11.7 Hz, 2H), 2.46−2.38 (4H, m) 2.29 (td, J = 11.7, 2.5 Hz, 2H), 1.99−1.89 (m, 2H), 1.88−1.82 (m, 2H), 1.42 (t, J = 7.0 Hz, 3H).

2-Methoxy-4-(1-methylpiperidin-4-yl)aniline (10b). **10b** was synthesized in 85% yield (yellow oil, 30 mg, 0.14 mmol) according to the same procedure as **10a**, from **9b** (600 mg, 2.32 mmol). HRMS (ESI +ve): found $[M]^+$ 221.1649 $[C_{13}H_{20}N_2O]^+$ requires 221.1648; δ_H (500 MHz, $CDCl_3$) 6.65−6.61 (m, 3H), 3.83 (s, 3H), 3.08 (dt, J =

12.1, 2.5 Hz, 2H), 2.46−2.37 (m, 1H), 2.38 (s, 3H), 2.16 (td, J = 12.1, 4.1 Hz, 2H), 1.91−1.81 (m, 4H).

(R)-Methyl 2-(Cyclopentylamino)butanoate (12a). (R)-Methyl 2-aminobutanoate **11a** (HCl salt, 1.50 g, 9.77 mmol) and cyclopentanone (0.87 mL, 9.77 mmol) were dissolved in DCE (0.1 M). The reaction was cooled to 0 °C, and NaOAc (801 mg, 9.77 mmol) and NaBH(OAc)$_3$ (4.14 g, 19.5 mmol) were added. The reaction was stirred at rt for 16 h. Upon completion, sat. NaHCO$_3$ was added and the aqueous phase was extracted with DCM (×3). The combined organic phases were washed with water, dried over MgSO$_4$, filtered, and concentrated in vacuo to afford compound **12a** as a yellow oil (1.45 g, 7.83 mmol, 80%). HRMS (ESI +ve): found [M]$^+$ 186.1498, [C$_{10}$H$_{20}$NO$_2$]$^+$ requires 186.1494; $[\alpha]_D^{21.8}$: −12.0 (c 1.0, MeOH); δ_H (500 MHz, CDCl$_3$): 3.73 (s, 3H), 3.22 (t, J = 6.6 Hz, 1H), 2.97 (quin, J = 6.7 Hz, 1H), 1.83−1.60 (m, 6H), 1.55−1.47 (m, 2H), 1.35−1.27 (m, 2H), 0.92 (t, J = 7.6 Hz, 3H).

(S)-Methyl 2-(Cyclopentylamino)butanoate (12b). **12b** was synthesized in 88% yield (brown oil, 1.42 g, 7.68 mmol) according to the same procedure as **12d**, from (S)-methyl 2-aminobutanoate **11b** (HCl salt, 1.34 g, 8.72 mmol) and cyclopentanone (0.78 mL, 8.72 mmol). HRMS (ESI +ve): found [M]$^+$ 186.1498, [C$_{10}$H$_{20}$NO$_2$]$^+$ requires 186.1494; $[\alpha]_D^{21.9}$: +11.8 (c 1.0, MeOH); δ_H (500 MHz, CDCl$_3$): 3.71 (s, 3H), 3.20 (t, J = 6.6 Hz, 1H), 2.96 (quin, J = 6.7 Hz, 1H), 1.83−1.58 (m, 6H), 1.55−1.47 (m, 2H), 1.35−1.27 (m, 2H), 0.91 (t, J = 7.6 Hz, 3H).

Methyl Cyclopentylglycinate (12c). **12c** was synthesized in 39% yield (yellow oil, 535 mg, 3.40 mmol) according to the same procedure as **12d**, from glycine methyl ester **11c** (HCl salt, 1.10 g, 8.77 mmol) and cyclopentanone (0.62 mL, 7.01 mmol). HRMS (ESI +ve): found [M]$^+$ 158.1176, [C$_8$H$_{15}$NO$_2$]$^+$ requires 158.1176; δ_H (500 MHz, CDCl$_3$): 3.73 (s, 3H), 3.42 (s, 2H), 3.07 (quin, J = 6.5 Hz, 1H), 1.85−1.77 (m, 2H), 1.75−1.66 (m, 2H), 1.60−1.50 (m, 2H), 1.40−1.32 (m, 2H).

(R)-Methyl 2-((3-Bromobenzyl)amino)butanoate (12d). **12d** was synthesized in 92% yield (yellow oil, 1.37 g, 4.79 mmol) according to the same procedure as **12a**, from (R)-methyl 2-aminobutanoate **11a** (HCl salt, 800 mg, 5.21 mmol) and 3-bromobenzaldehyde (0.61 mL, 5.21 mmol). HRMS (ESI +ve): found [M]$^+$ 286.0431, [C$_{12}$H$_{17}$BrNO$_2$]$^+$ requires 286.0437; $[\alpha]_D^{21.9}$: +22.9 (c 1.0, MeOH); δ_H (500 MHz, CDCl$_3$): 7.52 (t, J = 1.6 Hz, 1H), 7.38 (dt, J = 7.9, 1.6 Hz, 1H), 7.28−7.25 (m, 1H), 7.20−7.17 (m, 1H), 3.80 (d, J = 13.2 Hz, 1H), 3.74 (s, 3H), 3.60 (d, J = 13.2 Hz, 1H), 3.20 (t, J = 6.6 Hz, 1H), 1.76−1.62 (m, 2H), 0.96 (t, J = 7.6 Hz, 3H).

(R)-Methyl 2-(((3-Methylthiophen-2-yl)methyl)amino)butanoate (12e). **12e** was synthesized in 74% yield (yellow oil, 720 mg, 3.17 mmol) according to the same procedure as **12d**, from (R)-methyl 2-aminobutanote **11a** (HCl salt, 500 mg, 4.27 mmol) and 3-methylthiophene-2-carbaldehyde (0.46 mL, 4.27 mmol). HRMS (ESI +ve): found [M]$^+$ 228.1061, [C$_{11}$H$_{18}$NO$_2$S]$^+$ requires 228.1053; $[\alpha]_D^{22.6}$: +23.6 (c 1.0, MeOH); δ_H (500 MHz, CDCl$_3$): 7.10 (d, J = 5.0 Hz, 1H), 6.78 (d, J = 5.4 Hz, 1H), 3.93 (d, J = 13.9 Hz, 1H), 3.76−3.73 (m, 4H), 3.27 (t, J = 6.6 Hz, 1H), 2.17 (s, 3H), 1.74−1.62 (m, 2H), 0.95 (t, J = 6.9 Hz, 3H).

(R)-Methyl 2-(((4-Methylthiophen-2-yl)methyl)amino)butanoate (12f). **12f** was synthesized in 95% yield (yellow oil, 1.70 g, 7.48 mmol) according to the same procedure as **12d**, from (R)-methyl 2-aminobutanote **11a** (HCl salt, 1.20 mg, 7.81 mmol) and 4-methylthiophene-2-carbaldehyde (0.83 mL, 6.72 mmol). HRMS (ESI +ve): found [M]$^+$ 228.1062, [C$_{11}$H$_{18}$NO$_2$S]$^+$ requires 228.1053; $[\alpha]_D^{22.5}$: +28.4 (c 1.0, MeOH); δ_H (500 MHz, CDCl$_3$): 6.78 (t, J = 1.2 Hz, 1H), 6.73 (s, 1H), 3.98 (dd, J = 14.0, 0.8 Hz, 1H), 3.78 (dd, J = 14.0, 0.8 Hz, 1H), 3.74 (s, 3H), 3.29 (t, J = 6.5 Hz, 1H), 2.22 (d, J = 1.2 Hz, 3H), 1.74−1.62 (m, 2H), 0.95 (t, J = 7.6 Hz, 3H).

(R)-Methyl 2-(((5-Methylthiophen-2-yl)methyl)amino)butanoate (12g). **12g** was synthesized in 77% yield (yellow oil, 892 mg, 3.92 mmol) according to the same procedure as **12d**, from (R)-methyl 2-aminobutanote **11a** (HCl salt, 600 mg, 5.12 mmol) and 5-methylthiophene-2-carbaldehyde (0.43 mL, 4.10 mmol). HRMS (ESI +ve): found [M]$^+$ 228.1049, [C$_{11}$H$_{18}$NO$_2$S]$^+$ requires 228.1053; $[\alpha]_D^{22.2}$: +23.6 (c 1.0, MeOH); δ_H (500 MHz, CDCl$_3$):

6.68 (d, J = 3.2 Hz, 1H), 6.58−6.55 (m, 1H), 3.95 (d, J = 13.9 Hz, 1H), 3.75 (d, J = 13.9 Hz, 1H), 3.73 (s, 3H), 3.28 (t, J = 6.6 Hz, 1H), 2.45 (s, 3H), 1.89 (s, 1H), 1.74−1.61 (m, 2H), 0.94 (t, J = 6.9 Hz, 3H).

(R)-Methyl 2-((2-Chloro-5-nitropyrimidin-4-yl)(cyclopentyl)-amino)butanoate (13a). **12a** (700 mg, 3.78 mmol) and NaHCO$_3$ (635 mg, 7.6 mmol) were dissolved in cyclohexane (0.1 M) and stirred for 30 min. 2,4-Dichloro-5-nitropyrimidine (806 mg, 4.16 mmol) was added, and the reaction was stirred at 60 °C for 16 h. Upon completion, the reaction mixture was filtered, washed with CH$_2$Cl$_2$, and concentrated in vacuo. The residue was purified by Biotage column chromatography (cHex/EtOAc, 0−20%) to afford the title compound **13a** as a yellow solid (1.03 g, 2.99 mmol, 79%). HRMS (ESI +ve): found [M]$^+$ 343.1165, [C$_{14}$H$_{20}$ClN$_4$O$_4$]$^+$ requires 343.1173; $[\alpha]_D^{21.8}$: +228.5 (c 1.0, MeOH); δ_H (500 MHz, CDCl$_3$): 8.67 (s, 1H), 3.78−3.72 (m, 1H), 3.76 (s, 3H), 3.60−3.52 (m, 1H), 2.47−2.36 (m, 1H), 2.26−2.17 (m, 1H), 1.98−1.91 (m, 1H), 1.84−1.56 (m, 6H), 1.05 (t, J = 7.6 Hz, 3H).

(S)-Methyl 2-((2-Chloro-5-nitropyrimidin-4-yl)(cyclopentyl)-amino)butanoate (13b). **13b** was synthesized in 32% yield (yellow solid, 830 mg, 2.42 mmol) according to the same procedure as **13d**, from **12b** (1.40 g, 7.56 mmol) and 2,4-dichloro-5-nitropyrimidine (1.61 g, 8.31 mmol). HRMS (ESI +ve): found [M]$^+$ 343.1171, [C$_{14}$H$_{20}$ClN$_4$O$_4$]$^+$ requires 343.1173; $[\alpha]_D^{22.0}$: −229.9 (c 1.0, MeOH); δ_H (CDCl$_3$, 500 MHz): 8.67 (s, 1H), 3.78−3.72 (m, 1H), 3.76 (s, 3H), 3.60−3.51 (m, 1H), 2.46−2.36 (m, 1H), 2.25−2.17 (m, 1H), 2.09−2.01 (m, 1H), 1.99−1.90 (m, 1H), 1.84−1.47 (m, 6H), 1.05 (t, J = 7.6 Hz, 3H).

Methyl N-(2-Chloro-5-nitropyrimidin-4-yl)-N-cyclopentylglyci-nate (13c). **13c** was synthesized in 78% yield (yellow solid, 416 mg, 1.32 mmol) according to the same procedure as **13d**, from **12c** (265 mg, 1.69 mmol) and 2,4-dichloro-5-nitropyrimidine (360 mg, 1.85 mmol). HRMS (ESI +ve): found [M]$^+$ 315.0843, [C$_{12}$H$_{15}$ClN$_4$O$_4$]$^+$ requires 315.0860; δ_H (CDCl$_3$, 500 MHz): 8.65 (s, 1H), 4.17 (s, 2H), 3.98−3.88 (m, 1H), 3.79 (s, 3H), 2.16−2.07 (m, 2H), 1.78−1.70 (m, 2H), 1.64−1.53 (m, 4H).

(R)-Methyl 2-((3-Bromobenzyl)(2-chloro-5-nitropyrimidin-4-yl)-amino)butanoate (13d). **13d** was synthesized in 90% yield (yellow oil, 1.81 g, 4.08 mmol) according to the same procedure as **13a**, from **12d** (1.30 g, 4.54 mmol) and 2,4-dichloro-5-nitropyrimidine (970 mg, 5.00 mmol). HRMS (ESI +ve): found [M]$^+$ 443.0118, [C$_{16}$H$_{17}$BrClN$_4$O$_4$]$^+$ requires 443.0122; $[\alpha]_D^{22.0}$: +12.0 (c 1.0, MeOH); δ_H (500 MHz, CDCl$_3$): 8.64 (s, 1H), 7.45 (s, 1H), 7.41 (d, J = 7.8 Hz, 1H), 7.23 (d, J = 7.8 Hz, 1H), 7.17−7.13 (m, 1H), 4.75 (d, J = 15.8 Hz, 1H), 4.73−4.68 (m, 1H), 4.59 (d, J = 15.8 Hz, 1H), 3.82 (s, 3H), 2.32−2.23 (m, 1H), 2.10−2.00 (m, 1H), 1.07 (t, J = 7.4 Hz, 3H).

(R)-Methyl 2-((2-Chloro-5-nitropyrimidin-4-yl)((3-methylthio-phen-2-yl)methyl)amino)butanoate (13e). **13e** was synthesized in 90% yield (yellow solid, 1.18 g, 3.07 mmol) according to the same procedure as **13d**, from **12e** (770 mg, 3.39 mmol) and 2,4-dichloro-5-nitropyrimidine (723 mg, 3.72 mmol). HRMS (ESI +ve): found [M]$^+$ 385.0732, [C$_{15}$H$_{17}$ClN$_4$O$_4$S]$^+$ requires 385.0732; $[\alpha]_D^{22.1}$: +4.85 (c 1.0, MeOH); δ_H (500 MHz, CDCl$_3$): 8.65 (s, 1H), 7.15 (d, J = 5.2 Hz, 1H), 6.70 (d, J = 5.2 Hz, H2), 4.92 (dd, J = 5.4, 4.1 Hz, 1H), 4.75 (s, 2H), 3.80 (s, 3H), 2.30−2.20 (m, 1H), 2.16 (s, 3H), 2.07−2.00 (m, 1H), 1.09 (t, J = 7.4 Hz, 3H).

(R)-Methyl 2-((2-Chloro-5-nitropyrimidin-4-yl)((4-methylthio-phen-2-yl)methyl)amino)butanoate (13f). **13f** was synthesized in 81% yield (yellow solid, 2.32 g, 6.03 mmol) according to the same procedure as **13d**, from **12f** (1.70 g, 7.48 mmol) and 2,4-dichloro-5-nitropyrimidine (1.60 g, 8.23 mmol). HRMS (ESI +ve): found [M]$^+$ 385.0738, [C$_{15}$H$_{17}$ClN$_4$O$_4$S]$^+$ requires 385.0732; $[\alpha]_D^{22.5}$: +5.54 (c 1.0, MeOH); δ_H (500 MHz, CDCl$_3$): 8.70 (s, 1H), 6.82−6.81 (m, 1H), 6.71 (s, 1H), 4.95−4.80 (m, 3H), 3.82 (s, 3H), 2.32−2.22 (m, 1H), 2.18 (s, 3H), 2.09−2.00 (m, 1H), 1.07 (t, J = 7.4 Hz, 3H).

(R)-Methyl 2-((2-Chloro-5-nitropyrimidin-4-yl)((5-methylthio-phen-2-yl)methyl)amino)butanoate (13g). **13g** was synthesized in 86% yield (yellow gum, 1.30 g, 3.38 mmol) according to the same procedure as **13d**, from **12g** (892 mg, 3.92 mmol) and 2,4-dichloro-5-

nitropyrimidine (837 mg, 4.31 mmol). HRMS (ESI +ve): found $[M]^+$ 385.0732, $[C_{15}H_{17}ClN_4O_4S]^+$ requires 385.0732; $[\alpha]_D^{22.4}$: −2.78 (c 1.0, MeOH); δ_H (500 MHz, CDCl₃): 8.68 (s, 1H), 6.67 (d, J = 2.5 Hz, 1H), 6.52 (d, J = 2.5 Hz, H2), 4.98−4.93 (m, 1H), 4.84 (d, J = 15.9 Hz, 1H), 4.81 (d, J = 15.9 Hz, 1H), 3.81 (s, 3H), 2.38 (s, 3H), 2.31−2.21 (m, 1H), 2.08−2.00 (m, 1H), 1.06 (t, J = 7.4 Hz, 3H).

(R)-2-Chloro-8-cyclopentyl-7-ethyl-7,8-dihydropteridin-6(5H)-one (14a). A mixture of 13a (1.00 g, 2.92 mmol) in AcOH (0.4 M) was heated to 100 °C. Iron powder (196 mg, 3.5 mmol) was added batchwise, and the reaction was stirred for 6 h. Upon completion, the mixture was filtered through celite, washed with MeOH, and concentrated in vacuo. The residue was purified by Biotage column chromatography (cHex/EtOAc, 0−40%) to afford the title compound 14a as a yellow solid (345 mg, 1.23 mmol, 25%). HRMS (ESI +ve): found $[M]^+$ 281.1163, $[C_{13}H_{18}ClN_4O]^+$ requires 281.1169; $[\alpha]_D^{22.1}$: −96.2 (c 1.0, MeOH); δ_H (500 MHz, CDCl₃): 9.39 (s, 1H), 7.68 (s, 1H), 4.37−4.29 (m, 1H), 4.21 (dd, J = 7.4, 3.6 Hz, 1H), 2.11−2.05 (m, 1H), 2.00−1.74 (m, 7H), 1.70−1.61 (m, 2H), 0.96 (t, J = 7.6 Hz, 3H).

(S)-2-Chloro-8-cyclopentyl-7-ethyl-7,8-dihydropteridin-6(5H)-one (14b). 14b was synthesized in 28% yield (yellow solid, 186 mg, 0.66 mmol) according to the same procedure as 14d, from 13b (815 mg, 2.38 mmol). HRMS (ESI +ve): found $[M]^+$ 281.1163, $[C_{13}H_{18}ClN_4O]^+$ requires 281.1169; $[\alpha]_D^{22.1}$: +95.3 (c 1.0, MeOH); δ_H (500 MHz, CDCl₃): 9.67 (s, 1H), 7.70 (s, 1H), 4.32 (quin, J = 8.4 Hz, 1H), 4.21 (dd, J = 7.3, 3.5 Hz, 1H), 2.12−2.04 (m, 1H), 2.00−1.73 (m, 7H), 1.70−1.60 (m, 2H), 0.94 (t, J = 7.6 Hz, 3H).

2-Chloro-8-cyclopentyl-7,8-dihydropteridin-6(5H)-one (14c). 14c was synthesized in 31% yield (orange solid, 101 mg, 0.40 mmol) according to the same procedure as 14d, from 13c (410 mg, 1.30 mmol). HRMS (ESI +ve): found $[M]^+$ 281.1163, $[C_{13}H_{18}ClN_4O]^+$ requires 281.1169; $[\alpha]_D^{22.1}$: +95.3 (c 1.0, MeOH); δ_H (500 MHz, CDCl₃): 7.98 (s, 1H), 7.60 (s, 1H), 6.15 (quin, J = 8.4 Hz, 1H), 4.11 (s, 2H), 1.98−1.89 (m, 2H), 1.80−1.57 (m, 6H).

(R)-2-Chloro-8-(3-bromobenzyl)-7-ethyl-7,8-dihydropteridin-6(5H)-one (14d). 14d was synthesized in 42% yield (orange solid, 387 mg, 1.01 mmol) according to the same procedure as 14a, from 13d (1.80 g, 4.06 mmol). HRMS (ESI +ve): found $[M]^+$ 383.0078, $[C_{15}H_{15}BrClN_4O]^+$ requires 383.0091; $[\alpha]_D^{22.0}$: −18.0 (c 1.0, MeOH); δ_H (500 MHz, CDCl₃): 9.33 (s, 1H), 7.71 (s, 1H), 7.48−7.45 (m, 1H), 7.45 (s, 1H), 7.26−7.23 (m, 2H), 5.62 (d, J = 15.1, 1H), 4.16−4.12 (m, 1H), 4.08 (d, J = 15.1, 1H), 2.05−1.97 (m, 1H), 1.96−1.86 (m, 1H), 0.91 (t, J = 7.4 Hz, 3H).

(R)-2-Chloro-7-ethyl-8-((3-methylthiophen-2-yl)methyl)-7,8-di-hydropteridin-6(5H)-one (14e). 14e was synthesized in 47% yield (orange solid, 380 mg, 1.17 mmol) according to the same procedure as 14d, from 13e (960 mg, 2.49 mmol). HRMS (ESI +ve): found $[M]^+$ 323.0724, $[C_{14}H_{15}ClN_4OS]^+$ requires 323.0728; $[\alpha]_D^{22.2}$: −11.1 (c 1.0, MeOH); δ_H (500 MHz, CDCl₃): 8.70 (s, 1H), 7.65 (s, 1H), 6.86 (d, J = 3.3 Hz, 1H), 6.63−6.61 (m, 1H), 5.55 (d, J = 15.5, 1H), 4.33−4.29 (m, 2H), 2.46 (s, 3H), 2.07−1.88 (m, 2H), 0.90 (t, J = 7.4 Hz, 3H).

(R)-2-Chloro-7-ethyl-8-((4-methylthiophen-2-yl)methyl)-7,8-di-hydropteridin-6(5H)-one (14f). 14f was synthesized in 42% yield (orange solid, 300 mg, 0.93 mmol) according to the same procedure as 14d, from 13f (860 mg, 2.23 mmol). HRMS (ESI +ve): found $[M]^+$ 323.0728, $[C_{14}H_{15}ClN_4OS]^+$ requires 323.0728; $[\alpha]_D^{22.8}$: −18.0 (c 1.0, MeOH); δ_H (500 MHz, CDCl₃): 7.73 (s, 1H), 6.86 (s, 1H), 6.83 (d, J = 1.0 Hz, 1H), 5.58 (d, J = 15.5, 1H), 4.32−4.28 (m, 2H), 2.23 (s, 3H), 2.07−1.99 (m, 1H), 1.97−1.86 (m, 1H), 0.89 (t, J = 7.4 Hz, 3H).

(R)-2-Chloro-7-ethyl-8-((5-methylthiophen-2-yl)methyl)-7,8-di-hydropteridin-6(5H)-one (14g). 14g was synthesized in 18% yield (orange solid, 200 mg, 0.62 mmol) according to the same procedure as 14d, from 13g (1.30 g, 3.38 mmol). HRMS (ESI +ve): found $[M]^+$ 323.0727, $[C_{14}H_{15}ClN_4OS]^+$ requires 323.0728; $[\alpha]_D^{22.5}$: +18.7 (c 1.0, MeOH); δ_H (500 MHz, CDCl₃): 9.20 (s, 1H), 7.69 (s, 1H), 7.18 (d, J = 5.2 Hz, 1H), 6.83 (d, J = 5.2 Hz, 1H), 5.64 (d, J = 15.5, 1H), 4.29 (d, J = 15.5 Hz, 1H), 4.24 (dd, J = 6.3, 3.5 Hz, 1H), 2.26 (s, 3H), 2.05−1.99 (m, 1H), 1.98−1.87 (m, 1H), 0.92 (t, J = 7.6 Hz, 3H).

(R)-2-Chloro-8-cyclopentyl-7-ethyl-5-methyl-7,8-dihydropteri-din-6(5H)-one (15a). 14a (200 mg, 0.72 mmol) was dissolved in DMF (0.1 M), methyl iodide (58 μL, 0.93 mmol) was added, and the mixture was cooled to −10 °C. NaH (22 mg, 0.93 mmol) was added, and the reaction was stirred for 16 h. Upon completion, ice was added and the aqueous phase was extracted with EtOAc (×3). The combined organic phases were washed with water, dried over MgSO₄, filtered, and concentrated in vacuo. The residue was purified by Biotage column chromatography (cHex/EtOAc, 0−20%) to afford the title compound 15a as a white solid (200 mg, 0.68 mmol, 71%). HRMS (ESI +ve): found $[M]^+$ 295.1321, $[C_{14}H_{20}ClN_4O]^+$ requires 295.1326; $[\alpha]_D^{21.4}$: −88.3 (c 1.0, MeOH); δ_H (500 MHz, CDCl₃): 7.62 (s, 1H), 4.41−4.29 (m, 1H), 4.25 (dd, J = 7.6, 3.5 Hz, 1H), 3.33 (s, 3H), 2.12−2.04 (m, 1H), 2.02−1.58 (m, 9H), 0.86 (t, J = 7.4 Hz, 3H).

(S)-2-Chloro-8-cyclopentyl-7-ethyl-5-methyl-7,8-dihydropteri-din-6(5H)-one (15b). 15b was synthesized in 95% yield (white solid, 180 mg, 0.61 mmol) according to the same procedure as 15d, from 14b (180 mg, 0.64 mmol) and methyl iodide (52 μL, 0.83 mmol). HRMS (ESI +ve): found $[M]^+$ 295.1321, $[C_{14}H_{20}ClN_4O]^+$ requires 295.1326; $[\alpha]_D^{21.5}$: +93.5 (c 1.0, MeOH); δ_H (500 MHz, CDCl₃): 7.65 (s, 1H), 4.37−4.28 (m, 1H), 4.23 (dd, J = 7.6, 3.8 Hz, 1H), 3.31 (s, 3H), 2.10−2.02 (m, 1H), 2.00−1.58 (m, 9H), 0.85 (t, J = 7.6 Hz, 3H).

2-Chloro-8-cyclopentyl-5-methyl-7,8-dihydropteridin-6(5H)-one (15c). 15c was synthesized in 59% yield (white solid, 53 mg, 0.20 mmol) according to the same procedure as 15d, from 14c (85 mg, 0.37 mmol) and methyl iodide (27 μL, 0.43 mmol). HRMS (ESI +ve): found $[M]^+$ 267.0995, $[C_{12}H_{15}ClN_4O]^+$ requires 267.1007; δ_H (500 MHz, CDCl₃): 7.67 (s, 1H), 5.14 (quin, J = 8.4 Hz, 1H), 4.13 (s, 2H), 4.37−4.28 (m, 1H), 3.33 (s, 3H), 1.97−1.91 (m, 2H), 1.81−1.65 (m, 4H), 1.64−1.56 (m, 2H).

(R)-8-(3-Bromobenzyl)-2-chloro-7-ethyl-5-methyl-7,8-dihydrop-teridin-6(5H)-one (15d). 15d was synthesized in 71% yield (yellow solid, 200 mg, 0.51 mmol) according to the same procedure as 15a, from 14d (270 mg, 0.71 mmol) and methyl iodide (58 μL, 0.92 mmol). HRMS (ESI +ve): found $[M]^+$ 395.0269, $[C_{16}H_{17}BrClN_4O]^+$ requires 395.0274; $[\alpha]_D^{22.1}$: +15.2 (c 1.0, MeOH); δ_H (500 MHz, CDCl₃): 7.73 (s, 1H), 7.48−7.44 (m, 2H), 7.25−7.22 (m, 2H), 5.62 (d, J = 15.1 Hz, 1H), 4.17 (dd, J = 6.3, 3.5 Hz, 1H), 4.09 (d, J = 15.1 Hz, 1H), 3.35 (s, 3H), 2.02−1.93 (m, 1H), 1.90−1.80 (m, 1H), 0.84 (t, J = 7.4 Hz, 3H).

(R)-2-Chloro-7-ethyl-5-methyl-8-(3-methylthiophen-2-yl)-7,8-di-hydropteridin-6(5H)-one (15e). 15e was synthesized in 48% yield (yellow solid, 186 mg, 0.55 mmol) according to the same procedure as 15d, from 14e (370 mg, 1.15 mmol) and methyl iodide (72 μL, 1.15 mmol). HRMS (ESI +ve): found $[M]^+$ 337.0901, $[C_{15}H_{17}ClN_4OS]^+$ requires 337.0884; $[\alpha]_D^{23.3}$: +6.9 (c 1.0, MeOH); δ_H (500 MHz, CDCl₃): 7.69 (s, 1H), 7.17 (d, J = 5.4 Hz, 1H), 6.83 (d, J = 5.4 Hz, 1H), 5.61 (d, J = 15.3 Hz, 1H), 4.29 (d, J = 15.3 Hz, 1H), 4.27 (dd, J = 6.6, 3.5 Hz, 1H), 3.32 (s, 3H), 2.25 (s, 3H), 2.03−1.93 (m, 1H), 1.91−1.81 (m, 1H), 0.84 (t, J = 7.6 Hz, 3H).

(R)-2-Chloro-7-ethyl-5-methyl-8-(4-methylthiophen-2-yl)-7,8-di-hydropteridin-6(5H)-one (15f). 15f was synthesized in 53% yield (yellow oil, 260 mg, 0.77 mmol) according to the same procedure as 15d, from 14f (470 mg, 1.46 mmol) and methyl iodide (19 μL, 1.90 mmol). HRMS (ESI +ve): found $[M]^+$ 337.0881, $[C_{15}H_{17}ClN_4OS]^+$ requires 337.0884; $[\alpha]_D^{23.3}$: +4.9 (c 1.0, MeOH); δ_H (500 MHz, CDCl₃): 7.69 (s, 1H), 6.86 (s, 1H), 6.82 (s, 1H), 5.56 (d, J = 15.5 Hz, 1H), 4.33−4.29 (2H, m), 3.31 (s, 3H), 2.22 (s, 3H), 2.03−1.95 (m, 1H), 1.91−1.84 (m, 1H), 0.81 (t, J = 7.4 Hz, 3H).

(R)-2-Chloro-7-ethyl-5-methyl-8-(5-methylthiophen-2-yl)-7,8-di-hydropteridin-6(5H)-one (15g). 15g was synthesized in 53% yield (yellow solid, 110 mg, 0.33 mmol) according to the same procedure as 15d, from 14g (200 mg, 0.62 mmol) and methyl iodide (39 μL, 0.62 mmol). HRMS (ESI +ve): found $[M]^+$ 337.0866, $[C_{15}H_{17}ClN_4OS]^+$ requires 337.0884; $[\alpha]_D^{23.5}$: +1.7 (c 1.0, MeOH); δ_H (500 MHz, CDCl₃): 7.69 (s, 1H), 6.85 (d, J = 3.5 Hz, 1H), 6.61−6.59 (m, 1H), 5.53 (d, J = 15.5 Hz, 1H), 4.33−4.29 (2H, m), 3.32 (s,

3H), 2.45 (s, 3H), 2.04−1.95 (m, 1H), 1.91−1.83 (m, 1H), 0.82 (t, J = 7.4 Hz, 3H).

(R)-8-*Cyclopentyl-7-ethyl-2-((2-methoxy-4-(1-methylpiperidin-4-yl)phenyl)amino)-5-methyl-7,8-dihydropteridin-6(5H)-one (16a).* To **15a** (25 mg, 80 μmol) and **10b** (18 mg, 80 μmol) in a solvent mixture of dioxane/EtOH/H$_2$O (1:1:1, 0.1 M) was added conc. HCl (24 μL, 110 μmol). The reaction was stirred at 120 °C for 48 h. Upon completion, the reaction mixture was partitioned between EtOAc and NaOH (1 M) and the aqueous layer was further extracted with EtOAc (×2). The organic phase was combined, dried over MgSO$_4$, and concentrated in vacuo. The residue was purified by Biotage column chromatography (DCM/20% amm. MeOH, 0−40%) and reverse phase column chromatography (water/MeOH, 0−100%) to afford **16a** as a yellow solid (9.0 mg, 19 μmol, 22%). HRMS (ESI +ve): found [M]$^+$ 479.3101, [C$_{27}$H$_{38}$N$_6$O$_2$]$^+$ requires 479.3129; $[\alpha]_D^{21.8}$: −9.1 (*c* 1.0, MeOH); δ_H (500 MHz, CDCl$_3$): 8.20 (d, J = 8.2 Hz, 1H), 7.88 (s, 1H), 7.61 (s, 1H), 6.80 (dd, J = 8.2, 1.9 Hz, 1H), 6.75 (d, J = 1.9 Hz, 1H), 4.42 (quin, J = 8.0 Hz, 1H), 4.21 (dd, J = 7.7, 3.6 Hz, 1H), 3.90 (s, 3H), 3.59 (d, J = 10.7 Hz, 2H), 3.31 (s, 3H), 2.75 (s, 3H), 2.77−2.67 (m, 3H), 2.27 (q, J = 12.5 Hz, 2H), 2.14−1.92 (m, 4H), 1.92−1.60 (m, 8H), 0.87 (t, J = 7.6 Hz, 3H).

(R)-4-*((8-Cyclopentyl-7-ethyl-5-methyl-6-oxo-5,6,7,8-tetrahydropteridin-2-yl)amino)-3-isobutoxy-N-(1-methylpiperidin-4-yl)benzamide (16b).* **16b** was synthesized in 28% yield (white solid, 7.0 mg, 12 μmol) according to the same procedure as **16h**, from **15a** (13 mg, 44 μmol) and **5a** (14 mg, 44 μmol). HRMS (ESI +ve): found [M]$^+$ 564.3652, [C$_{31}$H$_{45}$N$_7$O$_3$]$^+$ requires 564.3657; $[\alpha]_D^{20.8}$: −31.2 (*c* 1.0, MeOH); δ_H (500 MHz, CDCl$_3$): 8.55 (d, J = 8.4 Hz, 1H), 7.68 (s, 1H), 7.67 (s, 1H), 7.40 (d, J = 1.6 Hz, 1H), 7.22 (dd, J = 8.4, 1.6 Hz, 1H), 6.50 (d, J = 6.9 Hz, 1H), 4.40−4.32 (m, 1H), 4.23 (dd, J = 7.4, 3.3 Hz, 1H), 4.22−4.17 (m, 1H), 3.90 (d, J = 6.3 Hz, 2H), 3.41 (d, J = 10.4 Hz, 2H), 3.33 (s, 3H), 2.68 (t, J = 8.0 Hz, 2H), 2.33 (s, 3H), 2.26−1.65 (m, 15H), 1.09 (d, J = 6.6 Hz, 6H), 0.87 (t, J = 7.4 Hz, 3H).

(R)-4-*((8-Cyclopentyl-7-ethyl-5-methyl-6-oxo-5,6,7,8-tetrahydropteridin-2-yl)amino)-3-ethoxy-N-(1-methylpiperidin-4-yl)benzamide (16c).* **16c** was synthesized in 24% yield (white solid, 13 mg, 24 μmol) according to the same procedure as **16h**, from **15a** (30 mg, 102 μmol) and **5b** (28 mg, 102 μmol). HRMS (ESI +ve): found [M]$^+$ 536.3345, [C$_{29}$H$_{41}$N$_7$O$_3$]$^+$ requires 536.3349; $[\alpha]_D^{21.8}$: −62.3 (*c* 1.0, MeOH); δ_H (500 MHz, CDCl$_3$): 8.55 (d, J = 8.2 Hz, 1H), 7.73 (s, 1H), 7.68 (s, 1H), 7.41 (d, J = 1.9 Hz, 1H), 7.35 (dd, J = 8.3, 1.9 Hz, 1H), 6.56 (s, 1H), 4.52−4.44 (m, 1H), 4.28−4.18 (m, 4H), 3.50 (d, J = 10.4 Hz, 2H), 3.34 (s, 3H), 2.72−2.64 (m, 2H), 2.74 (s, 3H), 2.20−1.97 (m, 6H), 1.93−1.68 (m, 8H), 1.51 (t, J = 6.9 Hz, 3H), 0.88 (t, J = 7.4 Hz, 3H).

(S)-4-*((8-Cyclopentyl-7-ethyl-5-methyl-6-oxo-5,6,7,8-tetrahydropteridin-2-yl)amino)-3-ethoxy-N-(1-methylpiperidin-4-yl)benzamide (16d).* **16d** was synthesized in 42% yield (white solid, 23 mg, 43 μmol) according to the same procedure as **16h**, from **15b** (30 mg, 102 μmol) and **5b** (28 mg, 102 μmol). HRMS (ESI +ve): found [M]$^+$ 536.3329, [C$_{29}$H$_{41}$N$_7$O$_3$]$^+$ requires 536.3349; $[\alpha]_D^{21.8}$: +51.9 (*c* 1.0, MeOH); δ_H (500 MHz, CDCl$_3$): 8.55 (d, J = 8.2 Hz, 1H), 7.89 (s, 1H), 7.67 (s, 1H), 7.45 (d, J = 1.9 Hz, 1H), 7.35 (dd, J = 8.3, 1.9 Hz, 1H), 6.56 (s, 1H), 4.52−4.44 (m, 1H), 4.33−4.23 (m, 2H), 4.20 (q, J = 6.9 Hz, 2H), 3.50 (d, J = 10.4 Hz, 2H), 3.33 (s, 3H), 2.72−2.64 (m, 2H), 2.78 (s, 3H), 2.20−1.97 (m, 6H), 1.93−1.68 (m, 8H), 1.50 (t, J = 6.9 Hz, 3H), 0.88 (t, J = 7.6 Hz, 3H).

4-((8-Cyclopentyl-5-methyl-6-oxo-5,6,7,8-tetrahydropteridin-2-yl)amino)-3-ethoxy-N-(1-methylpiperidin-4-yl)benzamide (16e). **16e** was synthesized in 6.6% yield (white solid, 2.0 mg, 3.9 μmol) according to the same procedure as **16h**, from **15c** (16 mg, 60 μmol) and **5b** (16 mg, 57 μmol). HRMS (ESI +ve): found [M]$^+$ 508.3028, [C$_{29}$H$_{41}$N$_7$O$_3$]$^+$ requires 508.3031; δ_H (500 MHz, CDCl$_3$): 8.53 (d, J = 8.4 Hz, 1H), 7.69 (s, 1H), 7.63 (s, 1H), 7.41 (d, J = 1.8 Hz, 1H), 7.23 (dd, J = 8.4, 1.8 Hz, 1H), 5.91 (s, 1H), 5.16 (quin, J = 8.1 Hz, H3), 4.22 (q, J = 7.6 Hz, 2H), 4.09 (s, 2H), 4.03−3.94 (m, 1H), 3.33 (s, 3H), 2.88−2.80 (m, 2H), 2.32 (s, 3H), 2.20−2.15 (m, 2H), 2.06 (m, 2H), 2.01−1.93 (m, 2H), 1.84−1.58 (m, 8H), 1.52 (t, J = 7.6 Hz, 3H).

(R)-4-*((8-(3-Bromobenzyl)-7-ethyl-5-methyl-6-oxo-5,6,7,8-tetrahydropteridin-2-yl)amino)-3-ethoxy-N-(1-methylpiperidin-4-yl)benzamide (16f).* **16f** was synthesized in 53% yield (white solid, 55 mg, 86 μmol) according to the same procedure as **16h**, from **15d** (65 mg, 164 μmol) and **5b** (46 mg, 164 μmol). HRMS (ESI +ve): found [M]$^+$ 622.2302, [C$_{31}$H$_{38}$BrN$_7$O$_3$]$^+$ requires 636.2298; $[\alpha]_D^{22.1}$: +5.1 (*c* 1.0, MeOH); δ_H (500 MHz, CDCl$_3$): 8.23 (d, J = 8.5 Hz, 1H), 7.74 (s, 1H), 7.63 (s, 1H), 7.50 (t, J = 1.6 Hz, 1H), 7.44 (dt, J = 7.6, 1.6 Hz, 1H), 7.42 (d, J = 1.9 Hz, 1H), 7.28−7.20 (m, 2H), 7.14 (dd, J = 8.5, 1.9 Hz, 1H), 5.96 (d, J = 7.9 Hz, 1H), 5.51 (d, J = 15.8 Hz, 1H), 4.23−4.16 (m, 4H), 4.04−3.94 (m, 1H), 3.38 (s, 3H), 2.76−2.67 (m, 2H), 2.31 (s, 3H), 2.17 (t, J = 10.9 Hz, 2H), 2.09−2.01 (m, 2H), 2.00−1.93 (m, 1H), 1.89−1.80 (m, 1H), 1.63−1.58 (m, 2H) 1.49 (t, J = 7.1 Hz, 3H), 0.87 (t, J = 7.4 Hz, 3H).

(R)-4-*((8-Benzyl-7-ethyl-5-methyl-6-oxo-5,6,7,8-tetrahydropteridin-2-yl)amino)-3-ethoxy-N-(1-methylpiperidin-4-yl)benzamide (16g).* **16g** was synthesized in 46% yield (pale yellow solid, 4.0 mg, 7.2 μmol) according to the same procedure as **16i**, from **16f** (10 mg, 16 μmol). HRMS (ESI +ve): found [M]$^+$ 558.3161, [C$_{31}$H$_{39}$N$_7$O$_3$]$^+$ requires 558.3193; $[\alpha]_D^{21.9}$: −9.7 (*c* 1.0, MeOH); δ_H (500 MHz, CDCl$_3$): 8.45 (d, J = 8.5 Hz, 1H), 7.75 (s, 1H), 7.73 (s, 1H), 7.42 (d, J = 1.6 Hz, 1H), 7.40−7.29 (m, 6H), 6.61 (d, J = 8.2 Hz, 1H), 5.66 (d, J = 15.1 Hz, 1H), 4.28−4.19 (m, 4H), 4.18 (dd, J = 6.3, 3.5 Hz, 1H), 3.48 (d, J = 11.7 Hz, 2H), 3.37 (s, 3H), 2.80−2.72 (m, 2H), 2.73 (s, 3H), 2.20−2.12 (m, 4H), 2.01−1.92 (m, 1H), 1.91−1.82 (m, 1H), 1.51 (t, J = 6.9 Hz, 3H), 0.87 (t, J = 7.9 Hz, 3H).

(R)-8-*(3-Bromobenzyl)-2-((2-ethoxy-4-(1-methylpiperidin-4-yl)phenyl)amino)-7-ethyl-5-methyl-7,8-dihydropteridin-6(5H)-one (16h).* **16h** was synthesized in 29% yield (white solid, 30 mg, 51 μmol) according to the same procedure as **16a**, from **15d** (69 mg, 174 μmol) and **10a** (39 mg, 166 μmol). HRMS (ESI +ve): found [M]$^+$ 593.2209, [C$_{30}$H$_{38}$BrN$_6$O$_2$]$^+$ requires 593.2234; $[\alpha]_D^{23.7}$: +1.7 (*c* 1.0, MeOH); δ_H (500 MHz, CDCl$_3$): 8.13 (s, 1H), 7.96 (d, J = 8.2 Hz, 1H), 7.68 (s, 1H), 7.46−7.42 (m, 2H), 7.23−7.20 (m, 2H), 6.74−6.70 (m, 2H), 5.51 (d, J = 15.5 Hz, 1H), 4.19−4.13 (m, 2H), 4.11 (q, J = 6.9 Hz, 2H), 3.67−3.63 (m, 2H), 3.35 (s, 3H), 2.85−2.75 (m, 2H), 2.82 (s, 3H), 2.70−2.61 (m, 1H), 2.28 (q, J = 12.3 Hz, 2H), 2.05−1.94 (m, 3H), 1.90−1.80 (m, 1H), 1.47 (t, J = 6.9 Hz, 3H), 0.85 (t, J = 7.6 Hz, 3H).

(R)-8-*Benzyl-2-((2-ethoxy-4-(1-methylpiperidin-4-yl)phenyl)amino)-7-ethyl-5-methyl-7,8-dihydropteridin-6(5H)-one (16i).* A solution of **16h** (14 mg, 24 μmol) and 10% Pd·C (1.5 mg, 14 μmol) in MeOH (0.01 M) was stirred at rt under a hydrogen atmosphere (1 atm) for 1 h. The mixture was filtered through celite and washed with MeOH. The solvent was removed in vacuo, and the residue was purified by reverse phase column chromatography (water/MeOH, 0−100%) to give the title compound **16i** as a white solid (5.0 mg, 9.7 μmol, 41%). HRMS (ESI +ve): found [M]$^+$ 515.3114, [C$_{30}$H$_{40}$N$_6$O$_2$]$^+$ requires 515.3129; $[\alpha]_D^{23.7}$: +24.2 (*c* 1.0, MeOH); δ_H (500 MHz, CDCl$_3$): 8.22 (d, J = 8.8 Hz, 1H), 7.68 (s, 1H), 7.58 (s, 1H), 7.37−7.29 (m, 5H), 6.72 (d, J = 1.6 Hz, 1H), 6.70 (dd, J = 8.2, 1.6 Hz, 1H), 5.62 (d, J = 15.1 Hz, 1H), 4.18−4.15 (m, 3H), 4.11 (q, J = 7.2 Hz, 2H), 3.64 (d, J = 10.4 Hz, 2H), 3.34 (s, 3H), 2.73 (s, 3H), 2.73−2.58 (m, 3H), 2.25−2.15 (m, 2H), 2.02−1.92 (m, 3H), 1.90−1.81 (m, 1H), 1.48 (t, J = 6.9 Hz, 3H), 0.85 (t, J = 7.4 Hz, 3H).

(R)-2-*((2-Ethoxy-4-(1-methylpiperidin-4-yl)phenyl)amino)-7-ethyl-5-methyl-8-((3-methylthiophen-2-yl)methyl)-7,8-dihydropteridin-6(5H)-one (16j).* **16j** was synthesized in 9.4% yield (yellow solid, 6.0 mg, 11 μmol) according to the same procedure as **16h**, from **15e** (40 mg, 120 μmol) and **10a** (26 mg, 110 μmol). HRMS (ESI +ve): found [M]$^+$ 535.2828, [C$_{29}$H$_{39}$N$_6$O$_2$S]$^+$ requires 535.2850; $[\alpha]_D^{23.5}$: +7.6 (*c* 1.0, MeOH); δ_H (500 MHz, CDCl$_3$): 8.31 (d, J = 8.2 Hz, 1H), 7.67 (s, 1H), 7.64 (s, 1H), 7.15 (d, J = 5.0 Hz, 1H), 6.83 (d, J = 5.0 Hz, 1H), 6.78 (dd, J = 8.2, 1.6 Hz, 1H), 6.73 (d, J = 1.6 Hz, 1H), 5.63 (d, J = 15.1 Hz, 1H), 4.33 (d, J = 15.1 Hz, 1H), 4.19 (dd, J = 6.5, 3.6 Hz, 1H), 4.13 (q, J = 6.9 Hz, 2H), 3.57 (d, J = 9.1 Hz, 2H), 3.32 (s, 3H), 2.76−2.60 (m, 6H), 2.25 (s, 3H), 2.24−2.15 (m, 2H), 2.02−1.91 (m, 3H), 1.88−1.79 (m, 1H), 1.49 (t, J = 6.9 Hz, 3H), 0.85 (t, J = 7.4 Hz, 3H).

(R)-2-((2-Ethoxy-4-(1-methylpiperidin-4-yl)phenyl)amino)-7-ethyl-5-methyl-8-((4-methylthiophen-2-yl)methyl)-7,8-dihydropteridin-6(5H)-one (16k). **16k** was synthesized in 23% yield (yellow solid, 20 mg, 37 μmol) according to the same procedure as **16h**, from **15f** (55 mg, 163 μmol) and **10a** (36 mg, 155 μmol). HRMS (ESI +ve): found $[M]^+$ 535.2835, $[C_{29}H_{39}N_6O_2S]^+$ requires 535.2850; $[\alpha]_D^{22.6}$: +7.6 (c 1.0, MeOH); δ_H (500 MHz, CDCl$_3$): 8.34 (d, J = 8.2 Hz, 1H), 7.67 (s, 1H), 7.45 (s, 1H), 7.14 (d, J = 1.3 Hz, 1H), 6.85 (s, 1H), 6.82–6.76 (m, 3H), 5.61 (d, J = 15.5 Hz, 1H), 4.34 (d, J = 15.5 Hz, 1H), 4.25 (dd, J = 6.3, 3.5 Hz 1H), 4.11 (q, J = 6.9 Hz, 2H), 3.35–3.29 (m, 5H), 2.60 (s, 3H), 2.58–2.46 (m, 3H), 2.22 (s, 3H), 2.20–2.12 (m, 2H), 2.00–1.92 (m, 3H), 1.89–1.80 (m, 1H), 1.48 (t, J = 6.9 Hz, 3H), 0.85 (t, J = 7.6 Hz, 3H).

(R)-2-((2-Ethoxy-4-(1-methylpiperidin-4-yl)phenyl)amino)-7-ethyl-5-methyl-8-((5-methylthiophen-2-yl)methyl)-7,8-dihydropteridin-6(5H)-one (16l). **16l** was synthesized in 25% yield (yellow oil, 18 mg, 34 μmol) according to the same procedure as **16h**, from **15g** (45 mg, 134 μmol) and **10a** (30 mg, 127 μmol). HRMS (ESI +ve): found $[M]^+$ 535.2833, $[C_{29}H_{39}N_6O_2S]^+$ requires 535.2850; $[\alpha]_D^{23.6}$: +11.1 (c 1.0, MeOH); δ_H (500 MHz, CDCl$_3$): 8.34 (d, J = 8.2 Hz, 1H), 7.67 (s, 1H), 7.63 (s, 1H), 6.83 (d, J = 3.2 Hz, 1H), 6.79 (dd, J = 8.2, 1.9 Hz, 1H), 6.75 (d, J = 1.8 Hz, 1H), 6.60 (d, J = 3.2 Hz, 1H), 5.57 (d, J = 15.5 Hz, 1H), 4.43 (d, J = 15.5 Hz, 1H), 4.26 (dd, J = 6.2, 3.6 Hz, 1H), 4.14 (q, J = 6.9 Hz, 2H), 3.57 (d, J = 10.1 Hz, 2H), 3.32 (s, 3H), 2.73 (s, 3H), 2.73–2.61 (m, 3H), 2.44 (s, 3H), 2.25–2.15 (m, 2H), 2.02–1.92 (m, 3H), 1.89–1.80 (m, 1H), 1.60 (t, J = 6.9 Hz, 3H), 0.84 (t, J = 7.4 Hz, 3H).

(R)-Methyl 2-((2,4-Dimethoxybenzyl)amino)butanoate (17). **17** was synthesized in 97% yield (yellow oil, 27.0 g, 101 mmol) according to the same procedure as **12d**, from (R)-methyl 2-aminobutanoate **11a** (HCl salt, 16.0 g, 104 mmol) and 2,4-dimethoxybenzaldehye (17.3 g, 101 mmol). HRMS (ESI +ve): found $[M]^+$ 268.1541, $[C_{14}H_{21}NO_4]^+$ requires 268.1543; $[\alpha]_D^{23.9}$: +11.8 (c 1.0, MeOH); δ_H (500 MHz, CDCl$_3$): 7.13 (d, J = 7.9 Hz, 1H), 6.45–6.41 (m, 2H), 3.81 (s, 3H), 3.80 (s, 3H), 3.71 (d, J = 13.2 Hz, 1H), 3.67–3.74 (m, 4H), 3.21 (t, J = 6.5 Hz, 1H), 1.73–1.63 (m, 2H), 0.91 (t, J = 7.4 Hz, 3H).

(R)-Methyl 2-((2-Chloro-5-nitropyrimidin-4-yl)(2,4-dimethoxybenzyl)amino)butanoate (18). **18** was synthesized in 78% yield (yellow gum, 33.4 g, 78.6 mmol) according to the same procedure as **13d**, from **17** (27.0 g, 101 mmol) and 2,4-dichloro-5-nitropyrimidine **15** (21.6 g, 111 mmol). HRMS (ESI +ve): found $[M]^+$ 425.1211, $[C_{18}H_{21}ClN_4O_6]^+$ requires 425.1222; $[\alpha]_D^{23.7}$: −6.9 (c 1.0, MeOH); δ_H (500 MHz, CDCl$_3$): 8.65 (s, 1H), 7.04 (d, J = 8.2 Hz, 1H), 6.40–6.37 (m, 2H), 4.47–4.43 (m, 2H), 4.40 (d, J = 16.1 Hz, 1H), 3.79 (s, 3H), 3.71 (s, 3H), 3.62 (s, 3H), 2.28–2.18 (m, 1H), 2.07–1.99 (m, 1H), 1.05 (t, J = 7.4 Hz, 3H).

(R)-2-Chloro-8-(2,4-dimethoxybenzyl)-7-ethyl-7,8-dihydropteridin-6(5H)-one (19). A solution of **18** (13.0 g, 30.6 mmol), 10% Pt·C (597 mg, 3.06 mmol), and VO(acac)$_2$ (650 mg, 2.45 mmol) in THF (0.3 M) was stirred at rt under a hydrogen atmosphere (1 atm) for 48 h. The mixture was filtered through celite, and the solvent was removed in vacuo to give **19** as a brown solid (11.0 g, 30.3 mmol, 98%). HRMS (ESI +ve): found $[M]^+$ 363.1198, $[C_{17}H_{19}ClN_4O_3]^+$ requires 363.1218; $[\alpha]_D^{23.4}$: +15.2 (c 1.0, MeOH); δ_H (500 MHz, CDCl$_3$): 9.72 (1H), 7.65 (s, 1H), 7.30 (d, J = 9.1 Hz, 1H), 6.47–6.45 (m, 2H), 5.35 (d, J = 14.7 Hz, 2H), 4.28 (dd, J = 5.4, 4.4 Hz, 1H), 4.20 (d, J = 14.7 Hz, 1H), 3.80 (s, 6H), 2.03–1.94 (m, 2H), 0.94 (t, J = 7.3 Hz, 3H).

(R)-2-Chloro-8-(2,4-dimethoxybenzyl)-7-ethyl-5-methyl-7,8-dihydropteridin-6(5H)-one (20). **20** was synthesized in 86% yield (yellow oil, 9.66 g, 25.6 mmol) according to the same procedure as **15d**, from **19** (10.8 g, 29.8 mmol) and methyl iodide (2.42 mL, 38.7 mmol). HRMS (ESI +ve): found $[M]^+$ 377.1366, $[C_{18}H_{21}ClN_4O_3]^+$ requires 377.1375; $[\alpha]_D^{23.7}$: +35.3 (c 1.0, MeOH); δ_H (500 MHz, CDCl$_3$): 7.62 (s, 1H), 7.32 (d, J = 8.8 Hz, 1H), 6.47–6.45 (m, 2H), 5.34 (d, J = 14.5 Hz, 1H), 4.34 (dd, J = 6.3, 3.8 Hz, 1H), 4.20 (d, J = 14.7 Hz, 1H), 3.81 (s, 6H), 3.30 (s, 3H), 1.99–1.85 (m, 2H), 0.85 (t, J = 7.9 Hz, 3H).

(R)-2-Chloro-7-5-methyl-7,8-dihydropteridin-6(5H)-one (21). A solution of **20** (5.09 g, 13.5 mmol) in TFA (1.3 M) was stirred at 80 °C for 4 h. Upon completion, the reaction was concentrated in vacuo to remove the majority of the TFA. The remaining TFA was quenched with sat. NaHCO$_3$ until pH 7–8 was reached and extracted with DCM (×3). The organic layers were washed with brine, dried over MgSO4, filtered, and concentrated in vacuo. The residue was purified by Biotage column chromatography (DCM/MeOH, 0−15%) to give **21** as a brown solid (2.02 g, 8.91 mmol, 66%). HRMS (ESI +ve): found $[M]^+$ 227.0695, $[C_9H_{11}ClN_4O]^+$ requires 227.0694; $[\alpha]_D^{23.7}$: +35.3 (c 1.0, MeOH); δ_H (500 MHz, CDCl$_3$): 7.73 (s, 1H), 6.39 (s, 1H), 4.34 (dd, J = 6.3, 4.7 Hz, 1H), 3.34 (s, 3H), 2.03–1.87 (m, 2H), 0.99 (t, J = 7.4 Hz, 3H).

(R)-2-Chloro-8-(3-chlorobenzyl)-7-ethyl-5-methyl-7,8-dihydropteridin-6(5H)-one (22a). To a solution of **21** (50 mg, 0.22 mmol) in DMF (0.2 M) was added 1-(bromomethyl)-3-chlorobenzene (36 μL, 0.28 mmol). The mixture was cooled to −10 °C, NaH (12 mg, 0.50 mmol) was added, and then the mixture was stirred at rt for 18 h. Upon completion, ice was added and the reaction was partitioned between EtOAc and water. The aqueous layer was further extracted with EtOAc (×3). The combined organic phases were washed with water (×2), dried over MgSO$_4$, filtered, and concentrated in vacuo. The residue was purified by Biotage column chromatography (cHex/EtOAc, 0−20%) to give **22a** as an orange solid (51 mg, 0.15 mmol, 66%). HRMS (ESI +ve): found $[M]^+$ 351.0775, $[C_{16}H_{16}Cl_2N_4O]^+$ requires 351.0774; $[\alpha]_D^{23.6}$: −1.4 (c 1.0, MeOH); δ_H (500 MHz, CDCl$_3$): 7.73 (s, 1H), 7.32–7.28 (m, 3H), 7.20–7.18 (m, 1H), 5.62 (d, J = 15.1 Hz, 1H), 4.17 (dd, J = 6.2, 3.2 Hz, 1H), 4.08 (d, J = 15.1 Hz, 1H), 3.35 (s, 3H), 2.00–1.81 (m, 3H), 0.84 (t, J = 7.6 Hz, 3H).

(R)-3-((2-Chloro-7-ethyl-5-methyl-6-oxo-6,7-dihydropteridin-8(5H)-yl)methyl)benzonitrile (22b). **22b** was synthesized in 37% yield (white solid, 28 mg, 0.08 mmol) according to the same procedure as **22a**, from **21** (50 mg, 0.22 mmol) and 3-(bromomethyl)benzonitrile (35 μL, 0.28 mmol). HRMS (ESI +ve): found $[M]^+$ 341.1112, $[C_{17}H_{16}ClN_5O]^+$ requires 342.1116; $[\alpha]_D^{23.7}$: −1.4 (c 1.0, MeOH); δ_H (500 MHz, CDCl$_3$): 7.74 (s, 1H), 7.63–7.56 (m, 2H), 7.56 (d, J = 7.7 Hz, 1H), 7.47 (t, J = 7.7 Hz, 1H), 5.58 (d, J = 15.5 Hz, 1H), 4.18 (d, J = 15.5 Hz, 1H), 4.15 (dd, J = 6.5, 3.6 Hz, 1H), 3.35 (s, 3H), 2.01–1.94 (m, 1H), 1.87–1.78 (m, 1H), 0.83 (t, J = 7.6 Hz, 3H).

(R)-2-Chloro-7-ethyl-8-(3-methoxybenzyl)-5-methyl-7,8-dihydropteridin-6(5H)-one (22c). **22c** was synthesized in 65% yield (colorless oil, 50 mg, 0.14 mmol) according to the same procedure as **22a**, from **21** (50 mg, 0.22 mmol) and 3-methoxybenzyl bromide (39 μL, 0.28 mmol). HRMS (ESI +ve): found $[M]^+$ 347.1269, $[C_{17}H_{19}ClN_4O_2]^+$ requires 347.1269; $[\alpha]_D^{23.6}$: −9.7 (c 1.0, MeOH); δ_H (500 MHz, CDCl$_3$): 7.69 (s, 1H), 7.28−7.24 (m, 1H), 6.87−6.84 (m, 3H), 5.63 (d, J = 15.1 Hz, 1H), 4.19 (dd, J = 6.3, 3.5 Hz, 1H), 4.10 (d, J = 15.1 Hz, 1H), 3.79 (s, 3H), 3.35 (s, 3H), 2.00−1.93 (m, 1H), 1.93−1.81 (m, 1H), 0.82 (t, J = 7.6 Hz, 3H).

(R)-2-Chloro-8-(2-bromobenzyl)-7-ethyl-5-methyl-7,8-dihydropteridin-6(5H)-one (22d). **22d** was synthesized in 62% yield (orange solid, 87 mg, 0.22 mmol) according to the same procedure as **22a**, from **21** (80 mg, 0.35 mmol) and 1-(bromomethyl)-2-chloro-benzene (111 mg, 0.45 mmol). HRMS (ESI +ve): found $[M]^+$ 397.0250, $[C_{16}H_{16}BrClN_4O]^+$ requires 397.0274; $[\alpha]_D^{21.5}$: −20.1 (c 1.0, MeOH); δ_H (500 MHz, CDCl$_3$): 7.72 (s, 1H), 7.58 (dd, J = 7.8, 1.2 Hz, 1H), 7.36 (dd, J = 7.8, 1.7 Hz, 1H), 7.30 (m, 1H), 7.19 (m, 1H), 5.63 (d, J = 15.1 Hz, 1H), 4.33 (d, J = 15.1 Hz, 1H), 4.19 (dd, J = 6.3, 3.8 Hz, 1H), 3.35 (s, 3H), 1.98−1.86 (m, 2H), 0.87 (t, J = 7.6 Hz, 3H).

(R)-2-Chloro-8-(4-bromobenzyl)-7-ethyl-5-methyl-7,8-dihydropteridin-6(5H)-one (22e). **22e** was synthesized in 21% yield (white solid, 35 mg, 0.09 mmol) according to the same procedure as **22a**, from **21** (95 mg, 0.42 mmol) and 1-(bromomethyl)-4-chloro-benzene (83 μL, 0.50 mmol). HRMS (ESI +ve): found $[M]^+$ 397.0249, $[C_{16}H_{16}Cl_2N_4O]^+$ requires 397.0247; $[\alpha]_D^{22.3}$: −47.1 (c 1.0, MeOH); δ_H (500 MHz, CDCl$_3$): 7.71 (s, 1H), 7.47 (d, J = 8.5 Hz, 2H), 7.18 (d, J = 8.5 Hz, 2H), 5.52 (d, J = 15.1 Hz, 1H), 4.14 (dd, J = 6.3, 3.5 Hz, 1H), 4.10 (d, J = 15.1 Hz, 1H), 3.33 (s, 3H), 1.98−1.90 (m, 1H), 1.86−1.77 (m, 1H), 0.81 (t, J = 7.6 Hz, 3H).

(R)-2-Chloro-7-ethyl-5-methyl-8-((4-methylthiazol-5-yl)methyl)-7,8-dihydropteridin-6(5H)-one (22f). **22f** was synthesized in 39% yield (white solid, 41 mg, 0.12 mmol) according to the same procedure as **22a**, from **21** (70 mg, 0.31 mmol) and 5-(chloromethyl)-4-methyl-1,3-thiazole (HCl salt, 68 mg, 0.37 mmol). HRMS (ESI +ve): found $[M]^+$ 338.0838, $[C_{14}H_{16}ClN_5OS]^+$ requires 338.0837; $[\alpha]_D^{22.7}$: −14.5 (c 1.0, MeOH); δ_H (500 MHz, CDCl$_3$): 8.68 (s, 1H), 7.71 (s, 1H), 5.46 (d, J = 15.5 Hz, 1H), 4.46 (d, J = 15.5 Hz, 1H), 4.27 (dd, J = 6.3, 3.5 Hz, 1H), 3.33 (s, 3H), 2.53 (s, 3H), 2.04−1.98 (m, 1H), 1.88−1.70 (m, 1H), 0.83 (t, J = 7.4 Hz, 3H).

(R)-8-(3-Chlorobenzyl)-2-((2-ethoxy-4-(1-methylpiperidin-4-yl)-phenyl)amino)-7-ethyl-5-methyl-7,8-dihydropteridin-6(5H)-one (23a). **23a** was synthesized in 13% yield (white solid, 8.0 mg, 15 μmol) according to the same procedure as **16h**, from **22a** (40 mg, 110 μmol) and **10a** (25 mg, 110 μmol). HRMS (ESI +ve): found $[M]^+$ 549.2727, $[C_{30}H_{37}ClN_6O_2]^+$ requires 549.2739; $[\alpha]_D^{23.1}$: +15.2 (c 1.0, MeOH); δ_H (500 MHz, CDCl$_3$): 8.16 (d, J = 8.2 Hz, 1H), 7.71 (s, 1H), 7.46 (s, 1H), 7.30−7.27 (m, 2H), 7.23−7.20 (m, 1H), 6.76−6.70 (m, 2H), 5.58 (d, J = 15.5 Hz, 1H), 4.18−4.09 (m, 4H), 3.50 (d, J = 11.0 Hz, 2H), 3.36 (s, 3H), 2.69 (s, 3H), 2.69−2.59 (m, 3H), 2.17 (q, J = 12.3 Hz, 2H), 2.00−1.91 (m, 3H), 1.88−1.80 (m, 1H), 1.47 (t, J = 7.6 Hz, 3H), 0.87 (t, J = 7.0 Hz, 3H).

(R)-3-((2-((2-Ethoxy-4-(1-methylpiperidin-4-yl)phenyl)amino)-7-ethyl-5-methyl-6-oxo-6,7-dihydropteridin-8(5H)-yl)methyl)-benzonitrile (23b). **23b** was synthesized in 10% yield (white solid, 6.6 mg, 12 μmol) according to the same procedure as **16h**, from **22b** (40 mg, 120 μmol) and **10a** (26 mg, 110 μmol). HRMS (ESI +ve): found $[M]^+$ 540.3071, $[C_{31}H_{37}N_7O_2]^+$ requires 540.3081; $[\alpha]_D^{24.0}$: −2.1 (c 1.0, MeOH); δ_H (500 MHz, CDCl$_3$): 8.08 (d, J = 8.2 Hz, 1H), 7.73 (s, 1H), 7.62−7.55 (m, 3H), 7.47 (t, J = 7.9 Hz, 1H), 7.41 (s, 1H), 6.73−6.69 (m, 2H), 5.55 (d, J = 15.5 Hz, 1H), 4.23 (d, J = 15.5 Hz, 1H), 4.14−4.07 (m, 3H), 3.44 (d, J = 11.7 Hz, 2H), 3.37 (s, 3H), 2.64 (s, 3H), 2.63−2.52 (m, 3H), 2.12 (q, J = 13.2 Hz, 2H), 2.00−1.91 (m, 3H), 1.86−1.77 (m, 1H), 1.46 (t, J = 6.9 Hz, 3H), 0.87 (t, J = 7.4 Hz, 3H).

(R)-8-(3-Methoxybenzyl)-2-((2-ethoxy-4-(1-methylpiperidin-4-yl)phenyl)amino)-7-ethyl-5-methyl-7,8-dihydropteridin-6(5H)-one (23c). **23c** was synthesized in 32% yield (yellow solid, 20 mg, 37 μmol) according to the same procedure as **16h**, from **22c** (40 mg, 120 μmol) and **10a** (26 mg, 110 μmol). HRMS (ESI +ve): found $[M]^+$ 545.3221, $[C_{31}H_{40}N_6O_3]^+$ requires 545.3235; $[\alpha]_D^{24.0}$: +13.2 (c 1.0, MeOH); δ_H (500 MHz, CDCl$_3$): 8.19 (d, J = 8.8 Hz, 1H), 7.71 (s, 1H), 7.67 (1H), 7.29−7.26 (m, 1H), 6.91 (d, J = 7.6 Hz, 1H), 6.88−6.84 (m, 2H), 6.75−6.72 (m, 2H), 5.61 (d, J = 15.1 Hz, 1H), 4.18−4.09 (m, 4H), 3.77 (s, 3H), 3.61 (d, J = 8.8 Hz, 2H), 3.34 (s, 3H), 2.80−2.69 (m, 2H), 2.75 (s, 3H), 2.67−2.60 (m, 1H), 2.19 (q, J = 12.4 Hz, 2h), 2.02−1.90 (m, 3H), 1.89−1.80 (m, 1H), 1.48 (t, J = 6.9 Hz, 3H), 0.85 (t, J = 7.6 Hz, 3H).

(R)-8-(2-Bromobenzyl)-2-((2-ethoxy-4-(1-methylpiperidin-4-yl)-phenyl)amino)-7-ethyl-5-methyl-7,8-dihydropteridin-6(5H)-one (23d). **23d** was synthesized in 13% yield (yellow solid, 7.1 mg, 12 μmol) according to the same procedure as **16h**, from **22d** (36 mg, 91 μmol) and **10a** (20 mg, 86 μmol). HRMS (ESI +ve): found $[M]^+$ 593.2210, $[C_{30}H_{37}BrN_6O_2]^+$ requires 593.2231; $[\alpha]_D^{22.0}$: −19.39 (c 1.0, MeOH); δ_H (500 MHz, CDCl$_3$): 8.06 (d, J = 8.8 Hz, 1H), 7.70 (s, 1H), 7.57 (d, J = 7.6 Hz, 1H), 7.52 (s, 1H), 7.29−7.26 (m, 2H), 7.19−7.16 (m, 1H), 6.72−6.70 (m, 2H), 5.41 (d, J = 16.1 Hz, 1H), 4.30 (d, J = 16.1 Hz, 1H), 4.15 (dd, J = 6.6, 3.8 Hz, 1H), 4.10 (q, J = 6.9 Hz, 2H), 3.54 (d, J = 10.7 Hz, 2H), 3.37 (s, 3H), 2.74−2.60 (m, 6H), 2.17 (m, 2H), 2.02−1.86 (m, 4H), 1.47 (t, J = 6.9 Hz, 3H).

(R)-8-(4-Bromobenzyl)-2-((2-ethoxy-4-(1-methylpiperidin-4-yl)-phenyl)amino)-7-ethyl-5-methyl-7,8-dihydropteridin-6(5H)-one (23e). **23e** was synthesized in 6% yield (yellow solid, 3.4 mg, 5.7 μmol) according to the same procedure as **16h**, from **22e** (35 mg, 89 μmol) and **10b** (20 mg, 84 μmol). HRMS (ESI +ve): found $[M]^+$ 593.2242, $[C_{30}H_{37}BrN_6O_2]^+$ requires 593.2234; $[\alpha]_D^{23.4}$: +6.2 (c 1.0, MeOH); δ_H (500 MHz, CDCl$_3$): 8.16 (d, J = 7.9 Hz, 1H), 7.69 (s, 1H), 7.59 (s, 1H), 7.47 (d, J = 8.2 Hz, 2H), 7.20 (d, J = 8.2 Hz, 2H), 6.74−6.69 (m, 2H), 5.51 (d, J = 15.5 Hz, 1H), 4.19−4.09 (m, 4H), 3.58 (d, J = 9.1 Hz, 2H), 3.34 (s, 3H), 2.74 (s, 3H), 2.75−2.59 (m,

3H), 2.19 (m, 2H), 2.02−1.90 (m, 3H), 1.85−1.76 (m, 1H), 1.47 (t, J = 6.9 Hz, 3H).

(R)-2-((2-Ethoxy-4-(1-methylpiperidin-4-yl)phenyl)amino)-7-ethyl-5-methyl-8-((4-methylthiazol-5-yl)methyl)-7,8-dihydropteri-din-6(5H)-one (23f). **23f** was synthesized in 31% yield (yellow solid, 17 mg, 32 μmol) according to the same procedure as **16h**, from **22f** (35 mg, 100 μmol) and **10a** (23 mg, 100 μmol). HRMS (ESI +ve): found $[M]^+$ 536.2787, $[C_{28}H_{37}N_7O_2S]^+$ requires 536.2802; $[\alpha]_D^{22.8}$: −8.3 (c 1.0, MeOH); δ_H (500 MHz, CDCl$_3$): 8.65 (s, 1H), 8.24 (d, J = 8.3 Hz, 1H), 7.69 (s, 1H), 7.64 (s, 1H), 6.77 (dd, J = 8.3, 1.8 Hz, 1H), 6.74 (d, J = 1.8 Hz, 1H), 5.47 (d, J = 15.8 Hz, 1H), 4.48 (d, J = 15.8 Hz, 1H), 4.17 (d, J = 6.5, 3.6 Hz, 1H), 4.13 (q, J = 7.0 Hz, 2H), 3.61 (d, J = 10.4 Hz, 2H), 3.32 (s, 3H), 2.75 (s, 3H), 2.75−2.70 (m, 2H), 2.66−2.63 (m, 1H), 2.52 (s, 3H), 2.26−2.15 (m, 2H), 2.03−1.94 (m, 3H), 1.86−1.76 (m, 1H), 1.49 (t, J = 7.0 Hz, 3H), 0.84 (t, J = 7.6 Hz, 3H).

ALK^{F1174L} Kinase Assay. ALK^{F1174L} activity was measured in a LanthaScreen Eu kinase binding assay. The assay was performed in 384-well plates containing ALK^{F1174L} enzyme (5 nM, Carna Biosciences), Kinase Tracer 236 (30 nM, Thermo Fisher Scientific), LanthaScreen Eu-anti-GST antibody (2 nM, Thermo Fisher Scientific), either 1% (v/v) dimethyl sulfoxide (DMSO) or the test compound (in the range from 0.5 nM to 100 μM in 1% (v/v) DMSO), and assay buffer (50 mM N-(2-hydroxyethyl)piperazine-N′-ethanesulfonic acid (HEPES) pH 7.5; 10 mM MgCl$_2$; 1 mM ethylene glycol-bis(β-aminoethyl ether)-N,N,N′,N′-tetraacetic acid and 0.01% (w/v) Brij-35; 1 mM dithiothreitol). The reaction was incubated for 60 min at room temperature. The plate was read on an EnVision multilabel plate reader (PerkinElmer, U.K.) calculating an emission ratio between the acceptor/tracer emission (665 nM) and the antibody/donor emission (615 nM). IC$_{50}$ values were determined using a nonlinear regression fit of the log(inhibitor concentration) versus emission ratio with a variable slope equation.

Bromodomain Thermal Shift. BRD4 thermal shift was measured in a differential scanning fluorimetry (DSF) assay. The assay was performed on a Stratagene Mx3005P system quantitative polymerase chain reaction (qPCR). The assay was performed in 96-well plates with 20 μL of protein at 2 μM in DSF-assay buffer (10 mM HEPES pH 7.5, 500 mM NaCl) to which 4 μL of Sypro orange dye and 0.4 μL of 10 μM compound in DMSO was added. The plate was sealed and centrifuged (1 min, 1000 rpm), and the qPCR machine was used to detect SYPRO fluorescence while increasing the temperature from 25 to 95 °C in 71 cycles. The sigmoidal part of the fluorescence signal was fitted using the Boltzmann equation, the points of change were defined, and the thermal shift was calculated by subtracting the protein/DMSO T_m shift from the protein/compound T_m shift.

BRD4 Isothermal Calorimetry. BRD4 activity was measured by isothermal calorimetry. The sample cell, sample syringe, and injection syringe were all equilibrated with gel filtration buffer (10 mM HEPES, 150 mM NaCl, 0.5 mM tris(2-carboxyethyl)phosphine (TCEP), 5% glycerol). The sample syringe was filled with compound solution (30−40 μM in gel filtration buffer), and the injection syringe was filled with protein solution (300 μM in gel filtration buffer). After equilibration of the machine, protein was injected over 21−30 injections, 8 μL each time. For the analysis of the data, the baseline and integration points were defined to determine binding heats. Data was fitted to the Boltzmann equation to determine thermodynamic parameters.

PLK-1 Kinase Assay. All PLK-1 IC$_{50}$s and percentage inhibitions at 10 and 100 nM were tested by Thermo Fisher Scientific in a Ź-LYTE activity assay using their SelectScreen biochemical kinase profiling service.

Kinase Selectivity Profiling. Compound X was assayed at 1 μM in the DiscoveRx KINOMEscan (*scan*EDGE) assay platform. The results for single-concentration binding interactions are reported as "%Ctrl" (DMSO = 100%Ctrl), where lower numbers indicate stronger hits.

Immunoassay and Immunoblotting. The human neuroblastoma Kelly cell line was maintained in RPMI with 10% fetal calf

serum. For dose–response experiments, cells were seeded into 10 cm dishes and, following attachment, treated with the indicated compound concentration in fresh media. After 3 h, the plates were transferred onto ice, the media were taken off, and the cells were washed once with ice-cold phosphate-buffered saline (PBS), before adding 5% CHAPS lysis buffer. After 20 min in lysis buffer, cells were scraped, transferred into Eppendorfs, and spun at 4 °C for 12 min at 12 000 rpm. The supernatant was transferred to a fresh tube, and the protein content was quantified using the Direct Detect system (Millipore). For ALK immunoassay analysis, 15 μg of protein per well was added in duplicate for each sample to measure either total or pY1586 ALK, and for immunoblotting, 5 μg of denatured lysates were loaded into 4−12% Bis/Tris gels, both according to previously published methods.[37]

Crystallization, Data collection, and Processing. Purified protein in 25 mM HEPES pH 7.5, 300 mM NaCl, 0.5 mM TCEP, 5% glycerol was cocrystallized with compounds in 1:3 molar ratio at 293 K using sitting drop vapor diffusion. Reservoir solutions contained 25% poly(ethylene glycol)3350, 0.2 M ammonium sulfate, 0.1 M Bis−Tris pH 6.5 or 30% pentaerythritol ethoxylate 15/4, 0.05 ammonium sulfate, 0.1 M Bis−Tris pH 6.5 respectively.

Diffraction data were collected at the SLS X06S overlaid with X-ray A and BESSY II 14.2 and processed using either XDS (PMID 20124692) or iMOSFLM (PMID 28569763). The data was scaled using aimless from the CCP4 suite (PMID 29533233) and phased with PHASER (PMID 28573584) using PDB ID 4OGI (PMID 24584101) as initial model. Manual model rebuilding alternated with structure refinement was performed in COOT (PMID 28291755) and REFMAC (PMID 15572771), respectively. Geometry of the final models was verified using MolProbity (PMID 29067766). Data collection and refinement statistics are summarized in Supp. Table 3.

NanoBRET Target Engagement Assay. The NanoBRET target engagement assay in principle was performed as described previously.[38,39] The full-length ALK and BRDBD1 plasmid containing C-terminal placements of NanoLuc were obtained by the manufacturer (Promega). To lower intracellular expression levels of the reporter fusion, the NanoLuc/kinase fusion construct was diluted into carrier DNA (pGEM3ZF-, Promega) at a mass ratio of 1:10 (mass/mass), prior to forming FuGENE HD complexes according to the manufacturer's instructions (Promega). DNA−FuGENE complexes were formed at a ratio of 1:3 (μg DNA/μL FuGENE). One part of the transfection complexes was then mixed with 20 parts (v/v) of HEK293T cells suspended at a density of 2×10^5/mL in Dulbecco's modified Eagle's medium (Gibco) + 10% fetal bovine serum (GE Healthcare), seeded into T75 flasks, and allowed to express for 20 h. For target engagement, both serially diluted test compound and NanoBRET Kinase Tracer K5 (ALK) and BRD-Tracer (BRD4BD1) (Promega) at a final concentration of 2 and 0.5 μM, respectively, were pipetted into white 96-well plates (Corning 3600). The corresponding ALK or BRD4BD1-transfected cells were added and reseeded at a density of 2×10^5/mL after trypsinization and resuspending in Opti-MEM without phenol red (Life Technologies). The system was allowed to equilibrate for 2 h at 37 °C/5% CO_2 prior to BRET measurements. To measure BRET, NanoBRET NanoGlo substrate + extracellular NanoLuc inhibitor (Promega) was added as per the manufacturer's protocol, and filtered luminescence was measured on a CLARIOstar plate reader (BMG Labtech) equipped with a 450 nm band-pass filter (donor) and a 610 nm low-pass filter (acceptor). Competitive displacement data were then graphed using GraphPad Prism 7 software using a four-parameter curve fit with the following equation: Y = bottom + (top − bottom)/$(1 + 10^{((\text{Log IC}_{50} - X) \times \text{HillSlope})})$.

Western Blot Analysis. Protein extracts of cells were prepared by lysis in radioimmunoprecipitation assay buffer (Sigma) supplemented with protease inhibitors (complete protease inhibitor cocktail, Roche). Protein extracts (25 μg) were separated by sodium dodecyl sulfate-polyacrylamide gel electrophoresis and transferred onto poly(vinylidene difluoride) membranes using the Trans-Blot Turbo transfer system (BioRad). After blocking with 5% bovine serum albumin in PBS with 0.1% Tween-20 for 30 min, the membrane was

incubated with primary antibodies for 1 h at room temperature. Horseradish peroxidase-linked secondary antibodies were incubated 30 min at room temperature followed by enhanced chemiluminescence (ECL) detection (ECL Western blot substrate, Pierce).

Antibodies. Primary antibodies were obtained from the following sources: PLK-1 (05-844) and phosphohistone H3 (Ser10) (05806) from Millipore; pPlk1-T210 (5472) from Cell Signaling; pPlk1-S137 (21738) from Abcam; and cyclin B1 (GNS1) and β-actin (A2228) from Sigma-Aldrich served as loading control.

Docking. Docking studies were performed using Glide, Schrödinger, LLC, New York, NY, 2018. Preparation of ALK using PDB codes 2XB7 was performed using Schrödinger Suite 2018-3 Protein Preparation Wizard; Epik, Schrödinger, LLC, New York, NY, 2018, and preparation of ligands was performed using LigPrep, Schrödinger, LLC, New York, NY, 2018.

■ ASSOCIATED CONTENT

Ⓢ Supporting Information

The Supporting Information is available free of charge on the ACS Publications website at DOI: 10.1021/acs.jmedchem.8b01947.

> Molecular formula strings (CSV)
> Tables with standard deviations for all compounds; data collection and refinement statistics for BRD4−ligand complexes with **16i** and **16k**; kinase and bromodomain selectivity profiling of **16k**; chiral shift NMR and HPLC experiments; and cell cycle analysis of BI-2536 and **16k** (PDF)

Accession Codes

The PDB codes for **16i** and **16k** bound to BRD4(1) are 6Q3Y and 6Q3Z, respectively.

■ AUTHOR INFORMATION

Corresponding Authors
*E-mail: Benjamin.Bellenie@icr.ac.uk. Phone: +44 (0) 2087224602 (B.B.).
*E-mail: Swen.Hoelder@icr.ac.uk. Phone: +44 (0) 2087224353 (S.H.).

ORCID Ⓞ
Stefan Knapp: 0000-0001-5995-6494
Swen Hoelder: 0000-0001-8636-1488

Notes
The authors declare no competing financial interest.

■ ACKNOWLEDGMENTS

■ ABBREVIATIONS

ALK, anaplastic lymphoma kinase; BET, bromo- and extra-terminal domain; BRD4, bromodomain 4; DMB, dimethoxybenzyl; INSR, insulin receptor; MSD, meso-scale discovery; MYCN, n-myc proto-oncogene protein; PLK, polo-like kinase

■ REFERENCES

(1) Park, J. R.; Eggert, A.; Caron, H. Neuroblastoma: Biology, Prognosis, and Treatment. *Pediatr. Clin. North Am.* 2008, 55, 97–120.

(2) Berry, T.; Luther, W.; Bhatnagar, N.; Jamin, Y.; Poon, E.; Sanda, T.; Pei, D.; Sharma, B.; Vetharoy, W. R.; Hallsworth, A.; Ahmad, Z.; Barker, K.; Moreau, L.; Webber, H.; Wang, W.; Liu, Q.; Perez-Atayde, A.; Rodig, S.; Cheung, N.-K.; Raynaud, F.; Hallberg, B.; Robinson, S. P.; Gray, N. S.; Pearson, A. D. J.; Eccles, S. A.; Chesler, L.; George, R. E. The ALKF1174L Mutation Potentiates the Oncogenic Activity of MYCN in Neuroblastoma. *Cancer Cell* 2012, 22, 117–130.

(3) Bresler, S. C.; Wood, A. C.; Haglund, E. A.; Courtright, J.; Belcastro, L. T.; Plegaria, J. S.; Cole, K.; Toporovskaya, Y.; Zhao, H.; Carpenter, E. L.; Christensen, J. G.; Maris, J. M.; Lemmon, M. A.; Mossé, Y. P. Differential Inhibitor Sensitivity of Anaplastic Lymphoma Kinase Variants Found in Neuroblastoma. *Sci. Transl. Med.* 2011, 3, No. 108ra114.

(4) Study Of Lorlatinib (PF-06463922) - NCT03107988.

(5) Puissant, A.; Frumm, S. M.; Alexe, G.; Bassil, C. F.; Qi, J.; Chanthery, Y. H.; Nekritz, E. A.; Zeid, R.; Gustafson, W. C.; Greninger, P.; Garnett, M. J.; McDermott, U.; Benes, C. H.; Kung, A. L.; Weiss, W. A.; Bradner, J. E.; Stegmaier, K. Targeting MYCN in Neuroblastoma by BET Bromodomain Inhibition. *Cancer Discovery* 2013, 3, 308–323.

(6) Delmore, J. E.; Issa, G. C.; Lemieux, M. E.; Rahl, P. B.; Shi, J.; Jacobs, H. M.; Kastritis, E.; Gilpatrick, T.; Paranal, R. M.; Qi, J.; Chesi, M.; Schinzel, A. C.; McKeown, M. R.; Heffernan, T. P.; Vakoc, C. R.; Bergsagel, P. L.; Ghobrial, I. M.; Richardson, P. G.; Young, R. A.; Hahn, W. C.; Anderson, K. C.; Kung, A. L.; Bradner, J. E.; Mitsiades, C. S. BET Bromodomain Inhibition as a Therapeutic Strategy to Target c-Myc. *Cell* 2011, 146, 904–917.

(7) Mertz, J. A.; Conery, A. R.; Bryant, B. M.; Sandy, P.; Balasubramanian, S.; Mele, D. A.; Bergeron, L.; Sims, R. J. Targeting MYC Dependence in Cancer by Inhibiting BET Bromodomains. *Proc. Natl. Acad. Sci.* 2011, 108, 16669–16674.

(8) Filippakopoulos, P.; Knapp, S. Targeting Bromodomains: Epigenetic Readers of Lysine Acetylation. *Nat. Rev. Drug Discovery* 2014, 13, 337–356.

(9) Barone, G.; Anderson, J.; Pearson, A. D. J.; Petrie, K.; Chesler, L. New Strategies in Neuroblastoma: Therapeutic Targeting of MYCN and ALK. *Clin. Cancer Res.* 2013, 19, 5814–5821.

(10) Peters, J.-U. Polypharmacology − Foe or Friend? *J. Med. Chem.* 2013, 56, 8955–8971.

(11) Amirouchene-Angelozzi, N.; Swanton, C.; Bardelli, A. Tumor Evolution as a Therapeutic Target. *Cancer Discovery* 2017, 7, 805–817.

(12) Patyar, S.; Prakash, A.; Medhi, B. Dual Inhibition: a Novel Promising Pharmacological Approach for Different Disease Conditions. *J. Pharm. Pharmacol.* 2011, 63, 459–471.

(13) Humphrey, R. W.; Brockway-Lunardi, L. M.; Bonk, D. T.; Dohoney, K. M.; Doroshow, J. H.; Meech, S. J.; Ratain, M. J.; Topalian, S. L.; Pardoll, D. M. Opportunities and Challenges in the Development of Experimental Drug Combinations for Cancer. *JNCI, J. Natl. Cancer Inst.* 2011, 103, 1222–1226.

(14) Ciceri, P.; Muller, S.; O'Mahony, A.; Fedorov, O.; Filippakopoulos, P.; Hunt, J. P.; Lasater, E. A.; Pallares, G.; Picaud, S.; Wells, C.; Martin, S.; Wodicka, L. M.; Shah, N. P.; Treiber, D. K.;

(15) Knapp, S. Dual Kinase-Bromodomain Inhibitors for Rationally Designed Polypharmacology. *Nat. Chem. Biol.* 2014, 10, 305–312.

(15) Ember, S. W. J.; Zhu, J.-Y.; Olesen, S. H.; Martin, M. P.; Becker, A.; Berndt, N.; Georg, G. I.; Schönbrunn, E. Acetyl-lysine Binding Site of Bromodomain-Containing Protein 4 (BRD4) Interacts with Diverse Kinase Inhibitors. *ACS Chem. Biol.* 2014, 9, 1160–1171.

(16) Dittmann, A.; Werner, T.; Chung, C.-W.; Savitski, M. M.; Fälth Savitski, M.; Grandi, P.; Hopf, C.; Lindon, M.; Neubauer, G.; Prinjha, R. K.; Bantscheff, M.; Drewes, G. The Commonly Used PI3-Kinase Probe LY294002 Is an Inhibitor of BET Bromodomains. *ACS Chem. Biol.* 2014, 9, 495–502.

(17) Andrews, F. H.; Singh, A. R.; Joshi, S.; Smith, C. A.; Morales, G. A.; Garlich, J. R.; Durden, D. L.; Kutateladze, T. G. Dual-activity PI3K−BRD4 Inhibitor for the Orthogonal Inhibition of MYC to Block Tumor Growth and Metastasis. *Proc. Natl. Acad. Sci.* 2017, 114, E1072−E1080.

(18) Gohda, J.; Suzuki, K.; Liu, K.; Xie, X.; Takeuchi, H.; Inoue, J.-i.; Kawaguchi, Y.; Ishida, T. BI-2536 and BI-6727, Dual Polo-like Kinase/Bromodomain Inhibitors, Effectively Reactivate Latent HIV-1. *Sci. Rep.* 2018, 8, No. 3521.

(19) Ember, S. W.; Lambert, Q. T.; Berndt, N.; Gunawan, S.; Ayaz, M.; Tauro, M.; Zhu, J.-Y.; Cranfill, P. J.; Greninger, P.; Lynch, C. C.; Benes, C. H.; Lawrence, H. R.; Reuther, G. W.; Lawrence, N. J.; Schönbrunn, E. Potent Dual BET Bromodomain-Kinase Inhibitors as Value-Added Multitargeted Chemical Probes and Cancer Therapeutics. *Mol. Cancer Ther.* 2017, 16, 1054–1067.

(20) Steegmaier, M.; Hoffmann, M.; Baum, A.; Lénárt, P.; Petronczki, M.; Kraššák, M.; Gürtler, U.; Garin-Chesa, P.; Lieb, S.; Quant, J.; Grauert, M.; Adolf, G. R.; Kraut, N.; Peters, J.-M.; Rettig, W. J. BI 2536, a Potent and Selective Inhibitor of Polo-like Kinase 1, Inhibits Tumor Growth In Vivo. *Curr. Biol.* 2007, 17, 316–322.

(21) Kothe, M.; Kohls, D.; Low, S.; Coli, R.; Rennie, G. R.; Feru, F.; Kuhn, C.; Ding, Y.-H. Research Article: Selectivity-determining Residues in Plk1. *Chem. Biol. Drug Des.* 2007, 70, 540–546.

(22) Galkin, A. V.; Melnick, J. S.; Kim, S.; Hood, T. L.; Li, N.; Li, L.; Xia, G.; Steensma, R.; Chopiuk, G.; Jiang, J.; Wan, Y.; Ding, P.; Liu, Y.; Sun, F.; Schultz, P. G.; Gray, N. S.; Warmuth, M. Identification of NVP-TAE684, a Potent, Selective, and Efficacious Inhibitor of NPM-ALK. *Proc. Natl. Acad. Sci.* 2007, 104, 270–275.

(23) Davis, M. I.; Hunt, J. P.; Herrgard, S.; Ciceri, P.; Wodicka, L. M.; Pallares, G.; Hocker, M.; Treiber, D. K.; Zarrinkar, P. P. Comprehensive Analysis of Kinase Inhibitor Selectivity. *Nat. Biotechnol.* 2011, 29, 1046–1051.

(24) Chen, L.; Yap, J. L.; Yoshioka, M.; Lanning, M. E.; Fountain, R. N.; Raje, M.; Scheenstra, J. A.; Strovel, J. W.; Fletcher, S. BRD4 Structure−Activity Relationships of Dual PLK1 Kinase/BRD4 Bromodomain Inhibitor BI-2536. *ACS Med. Chem. Lett.* 2015, 6, 764–769.

(25) Liu, S.; Yosief, H. O.; Dai, L.; Huang, H.; Dhawan, G.; Zhang, X.; Muthengi, A. M.; Roberts, J.; Buckley, D. L.; Perry, J. A.; Wu, L.; Bradner, J. E.; Qi, J.; Zhang, W. Structure-Guided Design and Development of Potent and Selective Dual Bromodomain 4 (BRD4)/Polo-like Kinase 1 (PLK1) Inhibitors. *J. Med. Chem.* 2018, 7785–7795.

(26) Marsilje, T. H.; Pei, W.; Chen, B.; Lu, W.; Uno, T.; Jin, Y.; Jiang, T.; Kim, S.; Li, N.; Warmuth, M.; Sarkisova, Y.; Sun, F.; Steffy, A.; Pferdekamper, A. C.; Li, A. G.; Joseph, S. B.; Kim, Y.; Liu, B.; Tuntland, T.; Cui, X.; Gray, N. S.; Steensma, R.; Wan, Y.; Jiang, J.; Chopiuk, G.; Li, J.; Gordon, W. P.; Richmond, W.; Johnson, K.; Chang, J.; Groessl, T.; He, Y.-Q.; Phimister, A.; Aycinena, A.; Lee, C. C.; Bursulaya, B.; Karanewsky, D. S.; Seidel, H. M.; Harris, J. L.; Michellys, P.-Y. Synthesis, Structure−Activity Relationships, and in Vivo Efficacy of the Novel Potent and Selective Anaplastic Lymphoma Kinase (ALK) Inhibitor 5-Chloro-N2-(2-isopropoxy-5-methyl-4-(piperidin-4-yl)phenyl)-N4-(2-(isopropylsulfonyl)phenyl)-pyrimidine-2,4-diamine (LDK378) Currently in Phase 1 and Phase 2 Clinical Trials. *J. Med. Chem.* 2013, 56, 5675–5690.

(27) Kinoshita, K.; Kobayashi, T.; Asoh, K.; Furuichi, N.; Ito, T.; Kawada, H.; Hara, S.; Ohwada, J.; Hattori, K.; Miyagi, T.; Hong, W.-

S.; Park, M.-J.; Takanashi, K.; Tsukaguchi, T.; Sakamoto, H.; Tsukuda, T.; Oikawa, N. 9-Substituted 6,6-Dimethyl-11-oxo-6,11-dihydro-5H-benzo[b]carbazoles as Highly Selective and Potent Anaplastic Lymphoma Kinase Inhibitors. *J. Med. Chem.* **2011**, *54*, 6286−6294.

(28) Huang, W.-S.; Liu, S.; Zou, D.; Thomas, M.; Wang, Y.; Zhou, T.; Romero, J.; Kohlmann, A.; Li, F.; Qi, J.; Cai, L.; Dwight, T. A.; Xu, Y.; Xu, R.; Dodd, R.; Toms, A.; Parillon, L.; Lu, X.; Anjum, R.; Zhang, S.; Wang, F.; Keats, J.; Wardwell, S. D.; Ning, Y.; Xu, Q.; Moran, L. E.; Mohemmad, Q. K.; Jang, H. G.; Clackson, T.; Narasimhan, N. I.; Rivera, V. M.; Zhu, X.; Dalgarno, D.; Shakespeare, W. C. Discovery of Brigatinib (AP26113), a Phosphine Oxide-Containing, Potent, Orally Active Inhibitor of Anaplastic Lymphoma Kinase. *J. Med. Chem.* **2016**, *59*, 4948−4964.

(29) Achary, R.; Mathi, G. R.; Lee, D. H.; Yun, C. S.; Lee, C. O.; Kim, H. R.; Park, C. H.; Kim, P.; Hwang, J. Y. Novel 2,4-Diaminopyrimidines Bearing Fused Tricyclic Ring Moiety for Anaplastic Lymphoma Kinase (ALK) Inhibitor. *Bioorg. Med. Chem. Lett.* **2017**, *27*, 2185−2191.

(30) Mathi, G. R.; Kang, C. H.; Lee, H. K.; Achary, R.; Lee, H.-Y.; Lee, J.-Y.; Ha, J. D.; Ahn, S.; Park, C. H.; Lee, C. O.; Hwang, J. Y.; Yun, C.-S.; Jung, H. J.; Cho, S. Y.; Kim, H. R.; Kim, P. Replacing the Terminal Piperidine in Ceritinib with Aliphatic Amines Confers Activities Against Crizotinib-resistant Mutants including G1202R. *Eur. J. Med. Chem.* **2017**, *126*, 536−549.

(31) Budin, G.; Yang, K. S.; Reiner, T.; Weissleder, R. Bioorthogonal Probes for Polo-like Kinase 1 Imaging and Quantification. *Angew. Chem., Int. Ed.* **2011**, *50*, 9378−9381.

(32) Baumeister, P.; Blaser, H.-U.; Studer, M. Strong Reduction of Hydroxylamine Accumulation in the Catalytic Hydrogenation of Nitroarenes by Vanadium Promoters. *Catal. Lett.* **1997**, *49*, 219−222.

(33) Filippakopoulos, P.; Qi, J.; Picaud, S.; Shen, Y.; Smith, W. B.; Fedorov, O.; Morse, E. M.; Keates, T.; Hickman, T. T.; Felletar, I.; Philpott, M.; Munro, S.; McKeown, M. R.; Wang, Y.; Christie, A. L.; West, N.; Cameron, M. J.; Schwartz, B.; Heightman, T. D.; La Thangue, N.; French, C. A.; Wiest, O.; Kung, A. L.; Knapp, S.; Bradner, J. E. Selective Inhibition of BET Bromodomains. *Nature* **2010**, *468*, 1067−1073.

(34) Mirguet, O.; Gosmini, R.; Toum, J.; Clément, C. A.; Barnathan, M.; Brusq, J.-M.; Mordaunt, J. E.; Grimes, R. M.; Crowe, M.; Pineau, O.; Ajakane, M.; Daugan, A.; Jeffrey, P.; Cutler, L.; Haynes, A. C.; Smithers, N. N.; Chung, C.-w.; Bamborough, P.; Uings, I. J.; Lewis, A.; Witherington, J.; Parr, N.; Prinjha, R. K.; Nicodème, E. Discovery of Epigenetic Regulator I-BET762: Lead Optimization to Afford a Clinical Candidate Inhibitor of the BET Bromodomains. *J. Med. Chem.* **2013**, *56*, 7501−7515.

(35) Fabian, M. A.; Biggs, W. H., III; Treiber, D. K.; Atteridge, C. E.; Azimioara, M. D.; Benedetti, M. G.; Carter, T. A.; Ciceri, P.; Edeen, P. T.; Floyd, M.; Ford, J. M.; Galvin, M.; Gerlach, J. L.; Grotzfeld, R. M.; Herrgard, S.; Insko, D. E.; Insko, M. A.; Lai, A. G.; Lélias, J.-M.; Mehta, S. A.; Milanov, Z. V.; Velasco, A. M.; Wodicka, L. M.; Patel, H. K.; Zarrinkar, P. P.; Lockhart, D. J. A Small Molecule−Kinase Interaction Map for Clinical Kinase Inhibitors. *Nat. Biotechnol.* **2005**, *23*, 329.

(36) Raab, M.; Krämer, A.; Hehlgans, S.; Sanhaji, M.; Kurunci-Csacsko, E.; Dötsch, C.; Bug, G.; Ottmann, O.; Becker, S.; Pachl, F.; Kuster, B.; Strebhardt, K. Mitotic Arrest and Slippage Induced by Pharmacological Inhibition of Polo-like Kinase 1. *Mol. Oncol.* **2015**, *9*, 140−154.

(37) Tucker, E. R.; Tall, J. R.; Danielson, L. S.; Gowan, S.; Jamin, Y.; Robinson, S. P.; Banerji, U.; Chesler, L. Immunoassays for the Quantification of ALK and Phosphorylated ALK Support the Evaluation of On-target ALK Inhibitors in Neuroblastoma. *Mol. Oncol.* **2017**, *11*, 996−1006.

(38) Vasta, J. D.; Corona, C. R.; Wilkinson, J.; Zimprich, C. A.; Hartnett, J. R.; Ingold, M. R.; Zimmerman, K.; Machleidt, T.; Kirkland, T. A.; Huwiler, K. G.; Ohana, R. F.; Slater, M.; Otto, P.; Cong, M.; Wells, C. I.; Berger, B.-T.; Hanke, T.; Glas, C.; Ding, K.; Drewry, D. H.; Huber, K. V. M.; Willson, T. M.; Knapp, S.; Müller, S.;

Meisenheimer, P. L.; Fan, F.; Wood, K. V.; Robers, M. B. Quantitative, Wide-Spectrum Kinase Profiling in Live Cells for Assessing the Effect of Cellular ATP on Target Engagement. *Cell Chem. Biol.* **2018**, *25*, 206.e11−214.e11.

(39) Machleidt, T.; Woodroofe, C. C.; Schwinn, M. K.; Méndez, J.; Robers, M. B.; Zimmerman, K.; Otto, P.; Daniels, D. L.; Kirkland, T. A.; Wood, K. V. NanoBRET—A Novel BRET Platform for the Analysis of Protein−Protein Interactions. *ACS Chem. Biol.* **2015**, *10*, 1797−1804.